Weierstraß-Institut
für Angewandte Analysis und Stochastik

Leibniz-Institut im Forschungsverbund Berlin e. V.

Preprint ISSN 2198-5855

Guaranteed upper bounds for the velocity error of pressure-robust Stokes discretisations

Philip Lukas Lederer[1], Christian Merdon [2]

submitted: August 17, 2020

[1] TU Wien
Institute for Analysis and Scientific Computing
Wiedner Hauptstraße 8-10
1040 Wien
Austria
E-Mail: philip.lederer@tuwien.ac.at

[2] Weierstrass Institute
Mohrenstr. 39
10117 Berlin
Germany
E-Mail: christian.merdon@wias-berlin.de

No. 2750
Berlin 2020

2010 *Mathematics Subject Classification.* 65N15, 65N30, 76D07, 76M10.

2008 *Physics and Astronomy Classification Scheme.* 47.10.ad, 47.11.Fg.

Key words and phrases. Incompressible Navier–Stokes equations, mixed finite elements, pressure-robustness, a posteriori error estimators, equilibrated fluxes, adaptive mesh refinement.

Edited by
Weierstraß-Institut für Angewandte Analysis und Stochastik (WIAS)
Leibniz-Institut im Forschungsverbund Berlin e. V.
Mohrenstraße 39
10117 Berlin
Germany

Fax: +49 30 20372-303
E-Mail: preprint@wias-berlin.de
World Wide Web: http://www.wias-berlin.de/

Guaranteed upper bounds for the velocity error of pressure-robust Stokes discretisations

Philip Lukas Lederer, Christian Merdon

ABSTRACT. This paper improves guaranteed error control for the Stokes problem with a focus on pressure-robustness, i.e. for discretisations that compute a discrete velocity that is independent of the exact pressure. A Prager-Synge type result relates the errors of divergence-free primal and $H(\mathrm{div})$-conforming dual mixed methods (for the velocity gradient) with an equilibration constraint that needs special care when discretised. To relax the constraints on the primal and dual method, a more general result is derived that enables the use of a recently developed mass conserving mixed stress discretisation to design equilibrated fluxes that yield pressure-independent guaranteed upper bounds for any pressure-robust (but not necessarily divergence-free) primal discretisation. Moreover, a provably efficient local design of the equilibrated fluxes is presented that reduces the numerical costs of the error estimator. All theoretical findings are verified by numerical examples which also show that the efficiency indices of our novel guaranteed upper bounds for the velocity error are close to 1.

1. INTRODUCTION

There is a long history of a posteriori error control for the Stokes problem [24, 40, 6, 1, 7, 32, 41] which which was only recently refined in [24] with a stronger focus on the possibility of pressure-independent error control for the velocity if the discretisation is pressure-robust. Pressure-robust discretisations were propagated in recent years and are characterised by a pressure-independent velocity error that avoids the error from the relaxation of the divergence constraint [18, 23, 25, 28, 21, 15, 42] and include divergence-free schemes like [39, 16, 12]. A similar decoupling is needed in a posteriori error control if one is interested in efficient bounds and appropriate mesh refinement for the velocity error for such methods. The residual-based approaches by [24, 19] achieve this by applying the curl operator to the residual, hence measuring only the error of the underlying vorticity equation.

In this paper we turn our interest now to guaranteed error control for the velocity and thereby refine existing approaches in [17, 34, 5, 27, 32]. In principle, the unified approach from e.g. [6, 17] rewrites many second order elliptic problems on some admissible domain Ω into the form

$$-\operatorname{div}\sigma = f \quad \text{on } \Omega \tag{1.1}$$

which is also possible, with $\sigma := \nu\nabla\boldsymbol{u} - pI_{d\times d}$, for the Stokes problem

$$\begin{aligned} -\nu\Delta\boldsymbol{u} + \nabla p &= \boldsymbol{f} \quad \text{on } \Omega,\\ \operatorname{div}(\boldsymbol{u}) &= 0 \quad \text{on } \Omega. \end{aligned}$$

Hence, the application of the whole a posteriori error estimators for (vector-valued) Poisson problems, in particular guaranteed upper bounds like [10, 30, 4, 11, 36, 13], also work for the Stokes problem. However, care has to be taken for the additional divergence constraint that often leads to pressure-dependent velocity error estimators or estimators for the combined velocity and pressure error. For problems of the form (1.1), there is the famous Prager-Synge theorem [35, 2] (originally for linear elasticity) that is nothing else than a Pythagoras theorem in L^2-norms, i.e.

$$\|\nabla(\boldsymbol{u}-\boldsymbol{v})\|^2 + \|\nabla\boldsymbol{u} - \nu^{-1}\sigma\|^2 = \|\nabla\boldsymbol{v} - \nu^{-1}\sigma\|^2,$$

where $\boldsymbol{u}$ can be understood as some approximation to $\boldsymbol{u}$ and σ only has to satisfy some orthogonality or equilibration constraint. In our Stokes setting it is required that $\boldsymbol{u}, \boldsymbol{v} \in \boldsymbol{V}_0$ and

$$\int_\Omega (\operatorname{div}\sigma + \boldsymbol{f})\cdot\boldsymbol{w}\,\mathrm{d}x = 0 \quad \text{for all } \boldsymbol{w} \in \boldsymbol{V}_0 \tag{1.2}$$

where $\boldsymbol{V}_0$ is the subspace of divergence-free $\boldsymbol{H}^1_0(\Omega)$ test functions. An important observation is that, opposite to the Poisson problem or linear elasticity where the constraint has to hold for the whole space $\boldsymbol{H}^1_0(\Omega)$, equation (1.2) is not equivalent to

$$\operatorname{div}(\sigma) + \boldsymbol{f} = 0.$$

DOI 10.20347/WIAS.PREPRINT.2750 Berlin 2020

Since $-\int qI : \nabla \boldsymbol{w} \,\mathrm{d}x = \int \nabla q \cdot \boldsymbol{w} \,\mathrm{d}x = 0$ for any $q \in H^1(\Omega)$ and $w \in \boldsymbol{V}_0$, the equilibration constraint and the stress σ can be gauged by any gradient force. Many equilibration error estimators, see e.g. [17] where unfortunately only $\nu = 1$ is examined, fix this gauging freedom by approximating the pseudo-stress $\tilde{\sigma} := \nabla \boldsymbol{u} - pI_{d\times d}$ or its discrete counterpart $\tilde{\sigma}_h \approx \nu \nabla \bar{\mathbf{u}}_h - \bar{p}_h I_{d\times d}$ with the equilibration constraint

$$\mathrm{div}(\tilde{\sigma}_h) + \boldsymbol{\pi}_k \boldsymbol{f} = 0$$

where $\boldsymbol{\pi}_k$ is the piecewise L^2 bestapproximation into the (vector-valued) polynomials of order k, and $\bar{\mathbf{u}}_h, \bar{p}_h$ are the discrete velocity and pressure solutions of an inf-sup stable discretisation of the Stokes equations. Their error estimator (for a divergence-free discretisation) then reads as

$$\|\nabla(\boldsymbol{u} - \bar{\boldsymbol{u}}_h)\|^2_{L^2(\Omega)} \leqslant \nu^{-1} \sum_{T\in\mathcal{T}} \left(\frac{h_T}{\pi} \|\boldsymbol{f} + \mathrm{div}(\tilde{\sigma}_h)\|_{L^2(T)} + \|\tilde{\sigma}_h - \bar{p}_h I_{d\times d} - \nu \nabla \bar{\mathbf{u}}_h\|_{L^2(T)} \right)^2 . \tag{1.3}$$

The seemingly innocent oscillations in the first term can have a severe effect in pressure-dominant situations, since

$$\nu^{-1}\|\boldsymbol{f} - \boldsymbol{\pi}_k \boldsymbol{f}\|_{L^2(\Omega)} \leqslant \nu^{-1}\|(\mathbf{id} - \boldsymbol{\pi}_k)\nabla p\|_{L^2(\Omega)} + \|(\mathbf{id} - \boldsymbol{\pi}_k)\Delta \boldsymbol{u}\|_{L^2(\Omega)}.$$

As one can see, there is a pressure-dependent term that can be relatively large for small ν. Even in a divergence-free setting $\bar{\mathbf{u}}_h \in \boldsymbol{V}_0$, where we are allowed to measure the oscillations after an application of the curl-operator, one would still end up with a term $\nu^{-1}\|h_T^2 \,\mathrm{curl}(\boldsymbol{\pi}_k \nabla p)\|_{L^2(\Omega)}$ that does not vanish and still produces an error of the same magnitude. To reduce this effect in classical equilibration procedures one would have to increase k which results in much more numerical costs and also assumes that the pressure is smooth enough.

To remove this dependency we propose a novel equilibration design that avoids the gauging issue altogether and ensures the equilibration condition (1.2) as it is for an $H(\mathrm{div})$-conforming subspace of $\boldsymbol{V}_0$. We so ensure that even after the discretisation of the equilibration constraint, the complete gauging freedom is preserved. This is done with the help of the recently developed mass conserving mixed stress formulation [15]. The resulting error estimator for a divergence-free discretisation structurally looks very similar to (1.3), but consists of the terms

$$\|\nabla(\boldsymbol{u} - \boldsymbol{u}_h)\|^2_{L^2(\Omega)} \leqslant \nu^{-1} \sum_{T\in\mathcal{T}} \left(c h_T^2 \|(\mathbf{id} - \boldsymbol{\pi}_s)\,\mathrm{curl}(\boldsymbol{f} + \mathrm{div}(\sigma_h))\|_{L^2(T)} + \|\mathrm{dev}(\sigma_h - \nu \nabla \boldsymbol{u}_h)\|_{L^2(T)} \right)^2 .$$

Note, that any gauging is not seen by the norms used on the right-hand side. The unfortunately unknown constant c stems from approximation properties of commuting interpolators and only depends on the shape of the cells in the triangulation. In the last part of the paper also a localized pressure-robust design for the equilibrated fluxes on node patches is presented.

The rest of the paper is organised as follows. Section 2 introduces the Stokes model problem and a Prager-Synge-type theorem. Section 3 recalls pressure-robust discretisations of the Stokes problem in the primal formulation and a dual mixed stress formulation. After shortly summarising classical equilibration error estimator approaches, Section 4 proves novel pressure-independent guaranteed upper bounds in the spirit of the Prager-Synge theorem but with relaxed constraints on primal and dual stress. A local design for equilibrated fluxes that fit into this framework is presented in Section 5. Section 6 is concerned with the efficiency of the new pressure-robust error estimators. Finally, Section 7 shows in several numerical examples that the novel upper bounds are indeed pressure-independent and allow very sharp error control and optimal adaptive mesh refinement for the velocity error of pressure-robust discretisations.

For the rest of this work we use a bold-face notation for vector valued functions and spaces, but stick to a standard notation for matrix valued functions and spaces to increase readability. We denote by $L^2(\Omega)$ the space of square integrable functions and by $H^s(\Omega)$ the standard Sobolev space with regularity s. Of special interestet is the H^1 space with homogeneous boundary conditions denoted by $H^1_0(\Omega)$.

Now let $\omega \subset \Omega$ be an arbitrary subset, then we use $\|\cdot\|_\omega$ for the L^2-norm on ω. In the case $\omega = \Omega$ we omit the notation for the domain and simply write $\|\cdot\|$. In a similar manner we denote by $(\cdot,\cdot)$ the L^2-inner product on Ω. For high order Sobolec spaces we use the standard notation, hence $\|\cdot\|_{H^s(\omega)}$ denotes the H^s-norm on ω, and as before, $\|\cdot\|_{H^s} = \|\cdot\|_{H^s(\Omega)}$.

Finally, the deviatoric part $\mathrm{dev}(A)$ of some matrix $A \in \mathbb{R}^{d\times d}$ is defined by

$$\mathrm{dev}(A) := A - \frac{\mathrm{tr}(A)}{d} I_{d\times d},$$

where $I_{d\times d}$ is the d-dimensional identity matrix, and $\mathrm{tr}(A) = \sum_{i=1}^{d} A_{ii}$ is the matrix trace.

2. The Stokes model problem and a Prager-Synge theorem

This section collects some preliminaries concerning the continuous Stokes problem and some important decompositions that allow to decouple velocity and pressure quantities.

2.1. **The Stokes model problem.** Given $\boldsymbol{f} \in L^2(\Omega)$ on some open, bounded domain $\Omega \subset \mathbb{R}^d$ $(d = 2, 3)$ with polygonal or polyhedral boundary, the Stokes problem with homogeneous boundary data seeks a velocity $\boldsymbol{u} \in \boldsymbol{V} := \boldsymbol{H}^1_0(\Omega)$ and some pressure $p \in Q := L^2_0(\Omega) = \{q_h \in L^2(\omega) : \int_\Omega p \,\mathrm{d}x\}$ with

$$\begin{aligned} -\nu\Delta\boldsymbol{u} + \nabla p &= \boldsymbol{f} \quad \text{on } \Omega, \\ \mathrm{div}(\boldsymbol{u}) &= 0 \quad \text{on } \Omega. \end{aligned}$$

The regularity assumptions of $\boldsymbol{u}$ and p above allow to expect a weak solution that satisfies

$$\begin{aligned} \nu(\nabla\boldsymbol{u}, \nabla\boldsymbol{v}) - (p, \mathrm{div}(\boldsymbol{v})) &= (\boldsymbol{f}, \boldsymbol{v}) \quad \text{for all } \boldsymbol{v} \in \boldsymbol{V}, \\ (q, \mathrm{div}(\boldsymbol{v})) &= 0 \qquad\quad \text{for all } q \in Q. \end{aligned}$$

Note, that the pressure acts as a Lagrange multiplier for the divergence constraint as the subspace of divergence-free functions is equal to

$$\boldsymbol{V}^0 := \{\boldsymbol{v} \in \boldsymbol{V} : \mathrm{div}(\boldsymbol{v}) = 0\} = \{\boldsymbol{v} \in \boldsymbol{V} : \forall q \in Q,\ (q, \mathrm{div}(\boldsymbol{v})) = 0\}.$$

A weak solution $\boldsymbol{u}$ or its stress $\sigma := \nu\nabla\boldsymbol{u}$ therefore can also be characterised by requiring $\boldsymbol{u} \in \boldsymbol{V}_0$ and

$$\nu(\nabla\boldsymbol{u}, \nabla\boldsymbol{v}) = (\sigma, \nabla\boldsymbol{v}) = (\boldsymbol{f}, \boldsymbol{v}) \quad \text{for all } \boldsymbol{v} \in \boldsymbol{V}_0.$$

2.2. **Characterising pressure-robustness.** Any force $\boldsymbol{f} \in \boldsymbol{L}^2(\Omega)$ can be uniquely decomposed into

$$\boldsymbol{f} = \nabla q + \mathbb{P}\boldsymbol{f}$$

with $q \in H^1(\Omega)/\mathbb{R}$ and the divergence-free Helmholtz–Hodge projector

$$\mathbb{P}\boldsymbol{f} \in \{\boldsymbol{v} \in L^2(\Omega)^d : (\boldsymbol{v}, \nabla w) = 0 \text{ for all } w \in H^1(\Omega)\}.$$

Due to $(\nabla q, \boldsymbol{v}) = (q, \mathrm{div}\,\boldsymbol{v}) = 0$ for all $\boldsymbol{v} \in \boldsymbol{V}_0$, $\boldsymbol{u}$ does not see the gradient force from this decomposition and it holds

$$\nu(\nabla\boldsymbol{u}, \nabla\boldsymbol{v}) = (\mathbb{P}\boldsymbol{f}, \boldsymbol{v}) \quad \text{for all } \boldsymbol{V}_0.$$

A discretisation that preserves this property, i.e. its discrete velocity solution is independent of any gradient force ∇q that is added to the right-hand side, is called pressure-robust, see [18, 28] for details.

2.3. **A Prager-Synge-type result for the Stokes system.** This section states a Pythagoras theorem for the Stokes system similar to that of Prager and Synge for the Poisson model problem and the linear elasticity problem [35, 2]. The Prager-Synge theorem relates the error of primal and equilibrated mixed approximations of the flux $\nabla\boldsymbol{u}$ (or $\epsilon(\boldsymbol{u})$ in elasticity) and gives rise to guaranteed error control by the design of equilibrated fluxes for these problems. The analogon in the context of the Stokes model problem for the flux of the velocity $\sigma := \nu\nabla\boldsymbol{u}$ reads as follows.

Theorem 2.1. Consider any $\boldsymbol{v} \in \boldsymbol{V}_0(\Omega)$ and any $\sigma \in H(\mathrm{div}, \Omega)$ and the equilibration constraint

$$\int_\Omega (\boldsymbol{f} + \mathrm{div}\, \sigma) \cdot \boldsymbol{v} \,\mathrm{d}x = 0 \quad \text{for all } \boldsymbol{v} \in \boldsymbol{V}_0. \tag{2.1}$$

Then, it holds the Pythagoras theorem

$$\|\nabla(\boldsymbol{u} - \boldsymbol{v})\|^2 + \|\nabla \boldsymbol{u} - \nu^{-1}\sigma\|^2 = \|\nabla \boldsymbol{v} - \nu^{-1}\sigma\|^2.$$

Proof. This follows directly from integration by parts and

$$\begin{aligned}\|\nabla(\boldsymbol{u} - \boldsymbol{v})\|^2 + \|\nabla \boldsymbol{u} - \nu^{-1}\sigma\|^2 - \|\nabla \boldsymbol{v} - \nu^{-1}\sigma\|^2 &= 2\int_\Omega (\nabla \boldsymbol{u} - \nu^{-1}\sigma) \cdot \nabla(\boldsymbol{u} - \boldsymbol{v}) \,\mathrm{d}x \\ &= 2\nu^{-1} \int_\Omega (\boldsymbol{f} + \mathrm{div}\, \sigma) \cdot (\boldsymbol{u} - \boldsymbol{v}) \,\mathrm{d}x = 0.\end{aligned}$$

□

Remark 2.2. Note, that the equilibration constraint (2.1) is pressure-independent, since $\int_\Omega \nabla q \cdot \boldsymbol{v} \,\mathrm{d}x = 0$ for all $\boldsymbol{v} \in \boldsymbol{V}_0$ and $q \in H^1(\Omega)$. Stronger constraints like $\boldsymbol{f} - \nabla q + \mathrm{div}(\sigma) = 0$ for some known pressure-approximation q are possible, but potentially lead to an dependency of $p - q$ somewhere, see Section 4.1.

Remark 2.3. In practise, both constraints on the function $\boldsymbol{v}$ and on the flux σ in Theorem 2.1 are hard to realise. Therefore, Section 4 derives guaranteed upper bounds for $\boldsymbol{v}$ that do not necessarily have to stem from a divergence-free (but pressure-robust) discretisation based on equilibrated fluxes σ that satisfy a discrete version of the equilibration property. Before that we recall previous results on how to obtain guaranteed upper bounds by equilibrated fluxes.

3. Pressure-robust finite element discretisations

This section recalls pressure-robust discretisations for the primal problem in velocity-pressure formulation and a pressure-robust discretisation of the dual mixed formulation. Note, that all discrete quantities related to the primal problem are marked with a bar on top.

3.1. Notation.

Consider some regular triangulation $\mathcal{T}$ of the domain Ω into regular simplices with vertices $\mathcal{V}$ and faces $\mathcal{F}$. The subset of interior faces is denoted by $\mathcal{F}(\Omega)$. The diameter of a simplex $T \in \mathcal{T}$ is given by h_T. We extend this notation in a similar manner onto faces and simply write h_F for the diameter of a face $F \in \mathcal{F}$. Further, if the triangulation is quasi uniform, we abbreviate the notation and simply write h for the maximum diameter of all simplices.

Let $F \in \mathcal{F}(\Omega)$ be some arbitrary face of an arbitrary element $T \in \mathcal{T}$. For the ease, we again denote by $\boldsymbol{n}$ the normal vector on F. Then,

$$\begin{aligned}\boldsymbol{a}_n &:= \boldsymbol{a} \cdot \boldsymbol{n}, \\ \boldsymbol{a}_t &:= \boldsymbol{a} - (\boldsymbol{a} \cdot \boldsymbol{n})\boldsymbol{n},\end{aligned}$$

denotes the scalar valued normal and the vector valued tangential part of some vector $\boldsymbol{a} \in \mathbb{R}^d$. Further, the brackets $[\![b]\!]_F$ denote the jump across the face of some (scalar or vector-valued) quantity b.

The space of piecewise (with respect to $\mathcal{T}$) polynomials of order k is denoted by $P_k(\mathcal{T})$ and the space of piecewise vector-valued polynomials of order k by $\boldsymbol{P}_k(\mathcal{T})$. The L^2-best approximation into $P_k(\mathcal{T})$ or $\boldsymbol{P}_k(\mathcal{T})$ these spaces read π_k or $\boldsymbol{\pi}_k$, respectively. We use the notation $P_{k,c}(\mathcal{T})$ to denote piecewise polynomials of order k that are continuous across element interfaces and extend the same notation to vector-valued polynomials. Next, the spaces

$$\begin{aligned}\mathrm{RT}_k(\mathcal{T}) &:= \{\boldsymbol{v}_h \in H(\mathrm{div}, \Omega) : \forall T \in \mathcal{T}\, \exists \boldsymbol{a}_T \in \boldsymbol{P}_k(T), b_T \in P_k(T),\, \boldsymbol{v}_h|_T(\boldsymbol{x}) = \boldsymbol{a}_T + b_T\boldsymbol{x}\}, \\ \mathrm{BDM}_k(\mathcal{T}) &:= \{\boldsymbol{v}_h \in H(\mathrm{div}, \Omega) : \forall T \in \mathcal{T}\, \boldsymbol{v}_h|_T \in \boldsymbol{P}_k(T)\},\end{aligned}$$

denote the space of Raviart-Thomas and Brezzi-Douglas-Marini functions of order $k \geqslant 0$, respectively. Further, let

$$\mathcal{N}_k(\mathcal{T}) := \{\boldsymbol{v}_h \in H(\mathrm{curl}, \Omega) : \forall T \in \mathcal{T}\, \exists \boldsymbol{a}_T \in \boldsymbol{P}_k(T), b_T \in P_k(T),\, \boldsymbol{v}_h|_T(\boldsymbol{x}) = \boldsymbol{a}_T + b_T \boldsymbol{x}^\perp\}$$

denote the space of Nédélec functions of order $k \geqslant 0$.

3.2. **Velocity-pressure formulation.** Consider an inf-sup stable pair of finite element spaces $\bar{\mathbf{V}}_h \subset \boldsymbol{V}$ and $\bar{Q}_h \subset Q$, and let $\mathcal{R}$ be some reconstruction operator that maps discretely divergence-free functions to exactly divergence-free ones, see equation (3.4) below. Note, that for simplicity, we only consider a discontinuous pressure approximation in this work, since this allows an element wise reconstruction operator. However we want to emphasize, that reconstruction operators for continuous pressure approximations are also possible but demand a more complicated construction, see [21].

The discrete solution $(\bar{\boldsymbol{u}}_h, \bar{p}_h) \in \bar{\boldsymbol{V}}_h \times \bar{Q}_h$ of the weak formulation of the Stokes problem is given by

$$\nu \int_\Omega \nabla \bar{\mathbf{u}}_h : \nabla \bar{\mathbf{v}}_h \,\mathrm{d}x - \int_\Omega \mathrm{div}(\bar{\mathbf{v}}_h)\bar{p}_h \,\mathrm{d}x = \int_\Omega \boldsymbol{f} \cdot \mathcal{R}(\bar{\mathbf{v}}_h)\,\mathrm{d}x \qquad \text{for all } \bar{\mathbf{v}}_h \in \bar{\mathbf{V}}_h \tag{3.1}$$

$$-\int_\Omega \mathrm{div}(\bar{\mathbf{u}}_h)\bar{q}_h \,\mathrm{d}x = 0 \qquad \text{for all } \bar{q}_h \in \bar{Q}_h. \tag{3.2}$$

Examples for suitable finite element spaces and corresponding reconstruction operators, i.e. standard $H(\mathrm{div})$-conforming interpolation operators, can be found in [18, 25, 26, 28]. For any divergence-free choice, like the Scott–Vogelius finite element, no reconstruction operator is needed and one can set $\mathcal{R} = \mathbf{id}$. See also Table 7.1 below in Section 7 for a list of elements that is used for our numerical experiments.

Some properties of the reconstruction operator are needed. Given the expected optimal convergence rate r of the Stokes solution, the reconstruction operator has to satisfy the properties

$$(\boldsymbol{f}, \bar{\mathbf{v}}_h - \mathcal{R}(\bar{\mathbf{v}}_h)) = (\boldsymbol{f} - \boldsymbol{\pi}_{r-2}\boldsymbol{f}, \bar{\mathbf{v}}_h - \mathcal{R}(\bar{\mathbf{v}}_h)) \quad \text{for all } \bar{\mathbf{v}}_h \in \bar{\mathbf{V}}_h, \tag{3.3}$$

that

$$\mathrm{div}(\mathcal{R}(\bar{\mathbf{v}}_h)) \in \bar{Q}_h \quad \text{and that} \quad (\mathrm{div}(\bar{\mathbf{v}}_h), \bar{q}_h) = (\mathrm{div}(\mathcal{R}(\bar{\mathbf{v}}_h)), \bar{q}_h) \quad \text{for all } \bar{\mathbf{v}}_h \in \bar{\mathbf{V}}_h, \bar{q} \in \bar{Q}_h. \tag{3.4}$$

Furthermore, we assume that the space of continuous affine vector fields is included in the velocity ansatz space, i.e $\boldsymbol{P}_{1,c} \subset \bar{\mathbf{V}}_h$ and that

$$\mathcal{R}(\bar{\mathbf{v}}_h) = \bar{\mathbf{v}}_h \quad \text{for all } \bar{\mathbf{v}}_h \in \boldsymbol{P}_{1,c}. \tag{3.5}$$

The following pressure robust a priori error estimate for the velocity can be expected, see [29] for quasi-optimal a priori error estimates under weaker regularity assumptions.

Theorem 3.1 (Pressure-robust a priori error estimates)**.** Given given $\boldsymbol{u} \in \boldsymbol{H}^m(\Omega) \cap \boldsymbol{V}$ with $m \geqslant 2$, it holds

$$\|\nabla(\boldsymbol{u} - \bar{\mathbf{u}}_h)\| \lesssim \inf_{\bar{\mathbf{v}}_h \in \bar{\mathbf{V}}_h} \|\nabla(\boldsymbol{u} - \bar{\mathbf{v}}_h)\| + h\|(\mathbf{id} - \boldsymbol{\pi}_{r-2})\Delta \boldsymbol{u}\| \lesssim h^s \|\boldsymbol{u}\|_{H^{s+1}}$$

where $s := \min\{m-1, r\}$.

3.3. **Mass conserving mixed stress formulation.** This section presents the recently developed mass conserving mixed stress (MCS) method from [15, 14, 22] that fits well into the Prager-Synge calculus as it satisfies a discrete version of the pressure-independent equilibration constraint (2.1). The MCS method was originally motivated by reformulating the continuous Stokes equations such that the exact solution $\boldsymbol{u}$ is an element of $H(\mathrm{div}, \Omega)$. Compared to the standard weak formulation this reads as a reduced regularity of the velocity. For the derivation of the mixed system, a new auxilliary variable σ is defined that should equal the gradient of the velocity. However, due to the reduced regularity of $\boldsymbol{u}$, this can only be incorporated in a weak sense. To this end one introduces a new function space

$$H(\mathrm{curl}\,\mathrm{div}, \Omega) := \{\sigma \in L^2(\Omega)^{d\times d} : \mathrm{div}(\sigma) \in (H_0(\mathrm{div}, \Omega))^\star, \mathrm{tr}(\sigma) = 0\},$$

where $(H_0(\mathrm{div},\Omega))^\star$ is the dual space of $H(\mathrm{div},\Omega))$ functions with vanishing normal trace. The condition $\mathrm{tr}(\sigma) = 0$ is related to the incompressibility constraint $\mathrm{tr}(\nabla \boldsymbol{u}) = \mathrm{div}(\boldsymbol{u}) = 0$. Using this space the equation "$\sigma = \nu\nabla\boldsymbol{u}$" for $\boldsymbol{u} \in H_0(\mathrm{div},\Omega))$ is then given by

$$\int_\Omega \frac{1}{\nu}\sigma : \tau \,\mathrm{d}x = -\langle \mathrm{div}(\tau), \boldsymbol{u}\rangle_{H_0(\mathrm{div},\Omega)} \quad \text{for all } \tau \in H(\mathrm{curl}\,\mathrm{div},\Omega),$$

where $\langle\cdot,\cdot\rangle_{H_0(\mathrm{div},\Omega)}$ is the standard duality pairing. For further details on the function spaces and the resulting mixed formulation in the continuous setting, we refer to [22]. The discrete counterpart is presented in the following.

For some given $k \geqslant 0$, the stress $\sigma \in H(\mathrm{curl}\,\mathrm{div},\Omega)$ is approximated in the space

$$\Sigma_h(\mathcal{T}) := \big\{\tau_h \in P_k(\mathcal{T})^{d\times d} : \mathrm{tr}(\tau_h) = 0, [\![(\tau_h)_{nt}]\!]_F = 0 \text{ for all } F \in \mathcal{F}(\Omega)\big\}.$$

Here $(\tau_h)_{nt}$ denotes the normal-tangential component of τ_h, i.e. $(\tau_h)_{nt} := (\tau_h\boldsymbol{n})_t$. Note, that $(\tau_h)_{nt}|_F$ lies in the tangent plane parallel to the face F. The other variables $\boldsymbol{u} \in \boldsymbol{V}$ and $p \in Q$ are discretised within the spaces

$$\boldsymbol{V}_h := \mathrm{RT}_k(\mathcal{T}) \quad \text{and} \quad Q_h := P_k(\mathcal{T}).$$

Then we seek a triplet $(\sigma_h^{\mathsf{MCS}}, \boldsymbol{u}_h, p_h) \in \Sigma_h \times \boldsymbol{V}_h \times Q_h$ such that

$$a(\sigma_h^{\mathsf{MCS}}, \tau_h) + \langle \mathrm{div}(\tau_h), \boldsymbol{u}_h\rangle_{\boldsymbol{V}_h} = (\nabla\bar{\boldsymbol{u}}_h, \tau_h) \qquad \text{for all } \tau_h \in \Sigma_h, \tag{3.6}$$

$$\langle \mathrm{div}(\sigma_h^{\mathsf{MCS}}), \boldsymbol{v}_h\rangle_{\boldsymbol{V}_h} + b_1(\boldsymbol{v}_h, p_h) = (-\boldsymbol{f}, \boldsymbol{v}_h) \qquad \text{for all } \boldsymbol{v}_h \in \boldsymbol{V}_h, \tag{3.7}$$

$$b_1(\boldsymbol{u}_h, q_h) = -b_1(\bar{\boldsymbol{u}}_h, q_h) \qquad \text{for all } q_h \in Q_h, \tag{3.8}$$

with the bilinearforms given by (note, that $\mathrm{tr}(\sigma_h) = 0$)

$$\begin{aligned}
a(\sigma_h, \tau_h) &:= \int_\Omega \frac{1}{\nu}\mathrm{dev}(\sigma_h) : \mathrm{dev}(\tau_h)\,\mathrm{d}x = \int_\Omega \frac{1}{\nu}\sigma_h : \tau_h \,\mathrm{d}x,\\
b_1(\boldsymbol{v}_h, q_h) &:= \int_\Omega \mathrm{div}(\boldsymbol{v}_h) q_h \,\mathrm{d}x,\\
\langle \mathrm{div}(\tau_h), \boldsymbol{v}_h\rangle_{\boldsymbol{V}_h} &:= \sum_{T\in\mathcal{T}} \int_T \mathrm{div}(\tau_h)\cdot\boldsymbol{v}_h \,\mathrm{d}x - \sum_{F\in\mathcal{F}} \int_F [\![(\tau_h)_{nn}]\!]\boldsymbol{v}_h\cdot\boldsymbol{n}\,\mathrm{d}s\\
&= -\sum_{T\in\mathcal{T}} \int_T \tau_h : \nabla\boldsymbol{v}_h \,\mathrm{d}x + \sum_{F\in\mathcal{F}} \int_F (\tau_h)_{nt}\cdot[\![(\boldsymbol{v}_h)_t]\!]\,\mathrm{d}s.
\end{aligned}$$

Note, that $\langle \mathrm{div}(\cdot),\cdot\rangle_{\boldsymbol{V}_h}$ reads as a discrete version of the duality pair $\langle \mathrm{div}(\cdot),\cdot\rangle_{H_0(\mathrm{div},\Omega)}$ for functions $\tau_h \in \Sigma_h$ and $\boldsymbol{v}_h \in \boldsymbol{V}_h$. This modification is essential since the discrete stress space is slightly non conforming, i.e. $\Sigma_h \not\subset H(\mathrm{curl}\,\mathrm{div})$. Now let $I_{\boldsymbol{V}_h}$ denote the standard interpolation operator into $\boldsymbol{V}_h$ and define for all $v_h \in \boldsymbol{V}_h$ the discrete H^1-like DG norm

$$\|v_h\|_{V_h}^2 := \sum_T \|\nabla v_h\|_T^2 + \sum_{F\in\mathcal{F}} \frac{1}{h_F}\|[\![v_h]\!]_t\|_F^2.$$

Theorem 3.2 (Pressure-robustness/Discrete equilibration constraint)**.** The discrete stress σ_h^{MCS} satisfies a discrete form of the equilibration constraint of Theorem 2.1 in the sense that

$$\langle \mathrm{div}(\sigma_h), I_{\boldsymbol{V}_h}\boldsymbol{V}_0\rangle_{\boldsymbol{V}_h} = (-\boldsymbol{f}, I_{\boldsymbol{V}_h}\boldsymbol{V}_0) = (-\mathbb{P}\boldsymbol{f}, I_{\boldsymbol{V}_h}\boldsymbol{V}_0).$$

Moreover, given $\boldsymbol{u} \in H^m(\Omega)^d$ and $\sigma \in H^{m-1}(\Omega)^{d\times d} \cap H^1(\Omega)^{d\times d}$ for some $m \geqslant 1$, it holds

$$\|\sigma - \sigma_h^{\mathsf{MCS}}\| \lesssim h^s\nu\|\boldsymbol{u}\|_{H^{s+1}}$$

where $s := \min\{m-1, k+1\}$.

Proof. The equilibration constraint follows from the second equation of the discrete system (3.6), since given any $\boldsymbol{v} \in \boldsymbol{V}_0$, testing with the divergence-free function $\boldsymbol{v}_h := I_{\boldsymbol{V}_h}\boldsymbol{v}$ leads to

$$\langle \mathrm{div}(\sigma_h^{\mathsf{MCS}}), \boldsymbol{v}_h\rangle_{\boldsymbol{V}_h} = (-\mathbb{P}\boldsymbol{f}, \boldsymbol{v}_h)$$

which is the claimed identity. We continue with the error estimate by showing that the solution of the best approximation problem (3.6) is related to solving a MCS-Stokes problem with a zero right-hand in the first and third equation. To this end let $\widetilde{\boldsymbol{u}}_h = \boldsymbol{u}_h + I_{\boldsymbol{V}_h}\bar{\boldsymbol{u}}_h$. Since $\operatorname{div}(\tau_h) \in P^{k-1}(T)^2$ for all $T \in \mathcal{T}$ and $[\![(\tau_h)_{nn}]\!] \in P^k(F)$ for all $F \in \mathcal{F}$, the properties of the Raviart-Thomas interpolator, integration by parts and the H^1-continuity of $\bar{\boldsymbol{u}}_h$ give

$$\begin{aligned}\langle \operatorname{div}(\tau_h), I_{\boldsymbol{V}_h}\bar{\boldsymbol{u}}_h\rangle_{\boldsymbol{V}_h} &= \sum_{T\in\mathcal{T}}\int_T \operatorname{div}(\tau_h)\cdot I_{\boldsymbol{V}_h}\bar{\boldsymbol{u}}_h \,\mathrm{d}x - \sum_{F\in\mathcal{F}}\int_F [\![(\tau_h)_{nn}]\!] I_{\boldsymbol{V}_h}\bar{\boldsymbol{u}}_h\cdot\boldsymbol{n}\,\mathrm{d}s\\ &= \sum_{T\in\mathcal{T}}\int_T \operatorname{div}(\tau_h)\cdot \bar{\boldsymbol{u}}_h \,\mathrm{d}x - \sum_{F\in\mathcal{F}}\int_F [\![(\tau_h)_{nn}]\!] \bar{\boldsymbol{u}}_h\cdot\boldsymbol{n}\,\mathrm{d}s\\ &= -\sum_{T\in\mathcal{T}}\int_T \tau_h : \nabla\bar{\boldsymbol{u}}_h \,\mathrm{d}x + \sum_{F\in\mathcal{F}}\int_F (\tau_h)_{nt}\cdot [\![(\bar{\boldsymbol{u}}_h)_t]\!]\,\mathrm{d}s = -(\nabla\bar{\boldsymbol{u}}_h,\tau_h).\end{aligned}$$

Further we have $b_1(I_{\boldsymbol{V}_h}\bar{\boldsymbol{u}}_h, q_h) = b_1(\bar{\boldsymbol{u}}_h, q_h)$ for all $q_h \in Q_h$. This shows that the triplet $(\sigma_h^{\mathsf{MCS}}, \widetilde{\boldsymbol{u}}_h, p_h) \in \Sigma_h \times \boldsymbol{V}_h \times Q_h$ solves the problem

$$\begin{aligned} a(\sigma_h^{\mathsf{MCS}},\tau_h) + \langle \operatorname{div}(\tau_h), \widetilde{\boldsymbol{u}}_h\rangle_{\boldsymbol{V}_h} &= 0 && \text{for all } \tau_h \in \Sigma_h,\\ \langle \operatorname{div}(\sigma_h^{\mathsf{MCS}}), \boldsymbol{v}_h\rangle_{\boldsymbol{V}_h} + b_1(\boldsymbol{v}_h, p_h) &= (-\boldsymbol{f},\boldsymbol{v}_h) && \text{for all } \boldsymbol{v}_h \in \boldsymbol{V}_h,\\ b_1(\widetilde{\boldsymbol{u}}_h, q_h) &= 0 && \text{for all } q_h \in Q_h.\end{aligned}$$

Since $\widetilde{\boldsymbol{u}}_h$ is exactly divergence free, the pressure robust error estimates of the standard Stokes problem from [22, 14] give

$$\nu\|I_{\boldsymbol{V}_h}\boldsymbol{u} - \widetilde{\boldsymbol{u}}_h\|_{V_h} + \|\sigma - \sigma_h^{\mathsf{MCS}}\| \lesssim h^s\nu\|\boldsymbol{u}\|_{H^{s+1}},$$

what concludes the proof. □

4. Relaxed pressure-robust guaranteed error control

In practise, both constraints on the function $\boldsymbol{v}$ and on the flux σ in Theorem 2.1 are hard to realise. Therefore we turn our interest to some relaxed version of this theorem that allows to estimate the error of any primal H^1-conforming discretisation (that is not necessarily divergence-free) by pressure-robust mixed methods like the MCS formulation from Section 3.3. In the first subsection a classical non-pressure-robust approach is revisited, while the second subsection presents novel guaranteed upper bounds that are pressure-independent (as long as the primal method is pressure-robust).

4.1. Revisiting classical non-pressure-robust equilibration.

In this section we shortly recall state-of-the-art equilibration error estimators for the Stokes problem from [17]. To compute a guaranteed error estimator in the spirit of Theorem 2.1, one is interested in a (discrete) stress σ that satisfies the equilibration constraint (approximately). A naive strategy to compute such an equilibrated flux is based on the mixed formulation of the Poisson model problem

$$\tilde{\sigma} = \nu\nabla\boldsymbol{u} - pI \quad \text{and} \quad \boldsymbol{f} + \operatorname{div}(\tilde{\sigma}) = 0.$$

In other words, the flux $\sigma := \tilde{\sigma} + pI$ is equilibrated in the sense of (2.1), because $\operatorname{div}(pI) = \nabla p$ has no influence in (2.1). In fact one could replace p by any other $q \in L^2(\Omega)$ or, if $p \in H^1(\Omega)$ can shift it into the equilibration constraint. In practise, see e.g. [17], one resorts to the choice $q = \bar{p}_h$, since p is unknown. Here, $\bar{p}_h$ is the discrete pressure solution of an inf-sup stable discretisation. This approach leads to the following guaranteed upper bound for the velocity error which is e.g. similar to [17, Theorem 4.1] for $q_1 = 0$ and $q_2 = \bar{p}_h$ or to [17, Corollary 5.1] for $q_1 = \bar{p}_h \in H^1(\Omega)$ and $q_2 = 0$.

Theorem 4.1. For a discrete Stokes solution $(\bar{\mathbf{u}}_h, \bar{p}_h) \in \boldsymbol{H}^1_0(\Omega) \times L^2_0(\Omega)$ of an inf-sup stable discretisation on some triangulation $\mathcal{T}$ with inf-sup constant $c_0 > 0$ and its discrete stress $\bar{\sigma}_h := \nu\nabla\bar{\mathbf{u}}_h$, and for any $\sigma_h \in$

$H(\mathrm{div},\Omega)$ with $\int_T f - \nabla q_1 + \mathrm{div}\,\sigma_h \,\mathrm{d}x = 0$ for any $T \in \mathcal{T}$ and for any $q_1 \in H^1(\Omega)$ and $q_2 \in L^2(\Omega)$, it holds

$$\|\boldsymbol{u} - \bar{\mathbf{u}}_h\|^2 \leqslant \nu^{-2} \sum_{T\in\mathcal{T}} \left(\frac{h_T}{\pi} \|\boldsymbol{f} - \nabla q_1 + \mathrm{div}(\sigma_h)\|_T + \|\sigma_h + q_2 I_{d\times d} - \bar{\sigma}_h\|_T \right)^2 + c_0^{-2} \|\,\mathrm{div}\,\bar{\mathbf{u}}_h\|^2.$$

Proof. The point of departure is the well-known error split [1, 17, 7]

$$\|\boldsymbol{u} - \bar{\mathbf{u}}_h\|^2 \leqslant \nu^{-2} \|\boldsymbol{r}\|^2_{\boldsymbol{V}_0^\star} + c_0^{-2} \|\,\mathrm{div}\,\bar{\mathbf{u}}_h\|^2$$

with the dual norm $\|\boldsymbol{r}\|_{\boldsymbol{V}_0^\star} := \sup_{\boldsymbol{v}\in\boldsymbol{V}_0\setminus\{0\}} \boldsymbol{r}(\boldsymbol{v})/\|\nabla\boldsymbol{v}\|$ of the residual

$$\begin{aligned}\boldsymbol{r}(\boldsymbol{v}) &= \int_\Omega \boldsymbol{f}\cdot\boldsymbol{v}\,\mathrm{d}x + \int_\Omega \bar{\sigma}_h : \nabla\boldsymbol{v}\,\mathrm{d}x \\ &= \int_\Omega (\boldsymbol{f} + \mathrm{div}(\sigma_h))\cdot\boldsymbol{v}\,\mathrm{d}x + \int_\Omega (\sigma_h - \bar{\sigma}_h) : \nabla\boldsymbol{v}\,\mathrm{d}x.\end{aligned}$$

Since $\int_T \nabla q_1 \cdot \boldsymbol{v}\,\mathrm{d}x = 0$, we can subtract the piecewise constant best-approximation $\boldsymbol{\pi}_0\boldsymbol{v}$ of $\boldsymbol{v}$ in the first term and employ piecewise Poincaré inequalities to obtain

$$\begin{aligned}\int_\Omega (\boldsymbol{f} - \nabla q_1 + \mathrm{div}(\sigma_h))\cdot\boldsymbol{v}\,\mathrm{d}x &= \int_\Omega (\boldsymbol{f} - \nabla q_1 + \mathrm{div}(\sigma_h))\cdot(\boldsymbol{v} - \boldsymbol{\pi}_0\boldsymbol{v})\,\mathrm{d}x \\ &\leqslant \sum_{T\in\mathcal{T}} \|\boldsymbol{f} - \nabla q_1 + \mathrm{div}(\sigma_h)\|_T \|\boldsymbol{v} - \boldsymbol{\pi}_0\boldsymbol{v}\|_T \\ &\leqslant \sum_{T\in\mathcal{T}} \frac{h_T}{\pi} \|\boldsymbol{f} - \nabla q_1 + \mathrm{div}(\sigma_h)\|_T \|\nabla\boldsymbol{v}\|_T.\end{aligned}$$

Since $\int q_2 I_{d\times d} : \nabla\boldsymbol{v}\,\mathrm{d}x = 0$, the second term is estimated by

$$\begin{aligned}\int_\Omega (\sigma_h - \bar{\sigma}_h) : \nabla\boldsymbol{v}\,\mathrm{d}x &= \int_\Omega (\sigma_h + q_2 I_{d\times d} - \bar{\sigma}_h) : \nabla\boldsymbol{v}\,\mathrm{d}x \\ &\leqslant \sum_{T\in\mathcal{T}} \|\sigma_h + q_2 I_{d\times d} - \bar{\sigma}_h\|_T \|\nabla\boldsymbol{v}\|_T.\end{aligned}$$

A Cauchy inequality concludes the proof. □

Remark 4.2 (Realisations)**.** A possible design of σ_h involves the Raviart-Thomas or Brezzi-Douglas-Marini finite element spaces of order k which is denoted by $\boldsymbol{V}_h$ and its divergence space denoted by Q_h. Then, one computes $\sigma_h^N \in (\boldsymbol{V}_h)^d$ and $\boldsymbol{u}_h \in (Q_h)^d$ such that

$$\begin{aligned}(\sigma_h^N, \tau_h) + (\boldsymbol{u}_h, \mathrm{div}(\tau_h)) &= (\bar{\sigma}_h - q_2 I_{d\times d}, \tau_h) && \text{for all } \tau_h \in (\boldsymbol{V}_h)^d \\ (v_h, \nu\,\mathrm{div}(\sigma_h^N)) &= -(\boldsymbol{f} - \nabla q_1, v_h) && \text{for all } v_h \in (Q_h)^d\end{aligned}$$

In practise, since the optimal q_1, q_2 are unknown, one usually takes the discrete pressure $q_1 = \bar{p}_h$ or $q_2 = \bar{p}_h$ depending on its regularity, which also enables local designs of equilibrated fluxes as detailed in e.g. [17] or using component-wise designs known for elliptic problems, see e.g. [10, 30, 4, 11, 36, 32, 13].

Remark 4.3 (Efficiency)**.** Efficiency is shown via equivalence to the classical explicit standard-residual error estimator, see [24] for a discussion when and why this is not efficient for pressure-robust discretisations in pressure-dominant situations. In the numerical examples below, we show that even the bestapproximation (which gives a lower bound for any local equilibration in the same space) strategy with $q_1 = 0$ and $q_2 = p_h$ is not efficient for the velocity error alone in a pressure-dominant situation. The only way to improve efficiency in these pressure-dependent designs is the pre-computation of a better pressure approximation as it has been suggested e.g. in [27]. However, in situations were the pressure is complicated or non-smooth this comes at highly increased numerical costs. Our novel pressure-robust local design of Section 5 has the advantage to be totally pressure-independent.

4.2. **Novel pressure-robust guaranteed upper bounds.** For the proof of the novel bounds we employ commuting interpolators whose properties are collected in the following theorem. Note, that the operator curl is different in two and three dimension and depends on the dimension of the quantity it is applied to. If applied to some scalar-valued quantity $\psi \in H^1(\Omega)$ it is defined by $\operatorname{curl}\psi := (\partial_{x_2}\psi, -\partial_{x_1}\psi)^T$. If applied to some vector-valued quantity $\boldsymbol{\psi} = (\psi_1, \psi_2) \in \boldsymbol{H}^1(\Omega)$ in $d = 2$ dimensions it reads $\operatorname{curl}\boldsymbol{\psi} := \partial_{x_1}\psi_2 - \partial_{x_2}\psi_1$, and if applied to some vector-valued quantity $\boldsymbol{\psi} \in H(\operatorname{curl}, \Omega)$ in $d = 3$ dimensions it reads $\operatorname{curl}\boldsymbol{\psi} := \nabla \times \boldsymbol{\psi}$.

Theorem 4.4 (Commuting interpolations)**.** Let $\boldsymbol{V}_h = \mathrm{RT}_k$ and $I_{\boldsymbol{V}_h}$ be its standard interpolation operator. Further we define

$$W_h^d := \begin{cases} P_{c,k+1} & \text{for } d = 2 \\ \mathcal{N}_k & \text{for } d = 3. \end{cases}$$

Now let $I_{W_h^d}$ be a mapping into W_h^d. For $d = 3$, the operator $I_{W_h^d}$ is the standard Nédélec interpolation operator as in [3], and for $d = 2$ we use the (corresponding commuting) H^1-interpolation operator as given in [33]. Let T be an arbitrary simplex and let F be an arbitrary face. The operators $I_{W_h^d}$ and $I_{\boldsymbol{V}_h}$ enjoy the properties:

1 For $d = 2$ we have the commuting property

$$I_{\boldsymbol{V}_h} \operatorname{curl}\psi = \operatorname{curl}(I_{W_h^2}\psi) \quad \text{for all } \psi \in H^2(\Omega), \tag{4.1}$$

and the approximation properties

$$\int_F (\mathbf{id} - I_{W_h^2})\psi \, q_h \,\mathrm{d}s = 0 \quad \text{for all } q_h \in P_{k-1}(F), \tag{4.2}$$

$$\int_T (\mathbf{id} - I_{W_h^2})\psi \, q_h \,\mathrm{d}s = 0 \quad \text{for all } q_h \in P_{k-2}(T), \tag{4.3}$$

$$\|\psi - I_{W_h^2}\psi\|_T \leqslant c_2 h_T \|\nabla\psi\|_T \quad \text{for all } \psi \in H^2(T). \tag{4.4}$$

2 For $d = 3$ we have the commuting property

$$I_{\boldsymbol{V}_h} \operatorname{curl}\boldsymbol{\psi} = \operatorname{curl}(I_{W_h^3}\boldsymbol{\psi}) \quad \text{for all } \boldsymbol{\psi} \in H^1(\operatorname{curl}, \Omega), \tag{4.5}$$

where $H^1(\operatorname{curl}, \Omega) = \{\boldsymbol{\psi} \in \boldsymbol{H}^1(\Omega) : \operatorname{curl}(\boldsymbol{\psi}) \in \boldsymbol{H}^1(\Omega)\}$, and the approximation properties

$$\int_F (\mathbf{id} - I_{W_h^3})\boldsymbol{\psi} \cdot (\boldsymbol{q}_h \times \boldsymbol{n}) \,\mathrm{d}s = 0 \quad \text{for all } \boldsymbol{q}_h \in \boldsymbol{P}_{k-1}(F), \tag{4.6}$$

$$\int_T (\mathbf{id} - I_{W_h^3})\boldsymbol{\psi} \cdot \boldsymbol{q}_h \,\mathrm{d}s = 0 \quad \text{for all } \boldsymbol{q}_h \in \boldsymbol{P}_{k-2}(T), \tag{4.7}$$

$$\|\boldsymbol{\psi} - I_{W_h^3}\boldsymbol{\psi}\|_T \leqslant c_2 h_T \|\nabla\boldsymbol{\psi}\|_T \quad \text{for all } \boldsymbol{\psi} \in H^1(\operatorname{curl}, T). \tag{4.8}$$

3 For $d = 2$ and $d = 3$ we have

$$\int_T (1 - I_{\boldsymbol{V}_h})\boldsymbol{v} \cdot \boldsymbol{q}_h \,\mathrm{d}x = 0 \quad \text{for all } v \in \boldsymbol{V}_0,\ \boldsymbol{q}_h \in \mathcal{N}_{k-2}(T) \tag{4.9}$$

$$\|\boldsymbol{v} - I_{\boldsymbol{V}_h}\boldsymbol{v}\|_T \leqslant c_1 h_T \|\nabla\boldsymbol{v}\|_T \quad \text{for all } \psi \in H^1(T), \tag{4.10}$$

with constants c_1, c_2 independent of h_T.

Proof. The properties of $I_{W_h^d}$ in two and three dimensions follows with the results in [33] and standard Bramble-Hilber arguments. Note, that in two dimensions, the results in [33] are only given for the rotated commuting diagram, i.e. $\nabla I_{W_h^2}\psi = I_{\mathcal{N}_k}(\nabla\psi)$, where$I_{\mathcal{N}_k}$ is the standard Nédélec interpolator . However, the claimed results in this work follow immediately since in two dimensions, the Raviat-Thomas space is simply a rotated Nédélec space and the curl is the rotated gradient, thus we have $(I_{\mathcal{N}_k}(\nabla\psi))^\perp = I_{\boldsymbol{V}_h}(\operatorname{curl}\psi)$. Similar results can be found in [9, 31, 3].

We continue with the proof of (4.9) but only present the case $d = 3$ since the two dimensional results follows with similar arguments. First observe that any divergence-free function $\boldsymbol{v} \in \boldsymbol{V}_0$ has a potential $\boldsymbol{v} = \operatorname{curl} \boldsymbol{\psi}$ for some $\boldsymbol{\psi} \in H^1(\operatorname{curl}, T)$. Then, for any $\boldsymbol{q}_h \in \mathcal{N}_{k-2}(T)$, (4.5) and integration by parts shows

$$\begin{aligned}\int_T (1 - I_{\boldsymbol{V}_h})\boldsymbol{v} \cdot \boldsymbol{q}_h \,\mathrm{d}x &= \int_T (1 - I_{\boldsymbol{V}_h}) \operatorname{curl} \boldsymbol{\psi} \cdot \boldsymbol{q}_h \,\mathrm{d}x \\ &= \int_T \operatorname{curl}((1 - I_{W_h^3})\boldsymbol{\psi}) \cdot \boldsymbol{q}_h \,\mathrm{d}x \\ &= \int_T (1 - I_{W_h^3})\boldsymbol{\psi} \cdot \operatorname{curl} \boldsymbol{q}_h \,\mathrm{d}x - \int_{\partial T} (1 - I_{W_h^3})\boldsymbol{\psi} \cdot (\boldsymbol{q}_h \times \boldsymbol{n}) \,\mathrm{d}s.\end{aligned}$$

Since $\boldsymbol{q}_h \in \mathcal{N}_{k-2}(T) \subset \mathcal{P}_{k-1}(T)$ and hence $\operatorname{curl} \boldsymbol{q}_h \in P_{k-2}(T)$ and $\boldsymbol{q}_h \cdot \boldsymbol{n}_F|_F \in P_{k-1}(F)$, the right-hand side vanishes due to (4.7) and (4.6). This concludes the proof. □

We are now in the position to derive pressure-robust guaranteed upper bounds via equilibrated fluxes with a proper discrete analogon of the equilibration constraint (2.1).

Theorem 4.5. Assume the regularity $\boldsymbol{f} \in H(\operatorname{curl}, \Omega)$. For the discrete stress $\bar{\sigma}_h := \nu \nabla \bar{\mathbf{u}}_h$ of the velocity-pressure formulation and any discrete stress $\sigma_h \in \Sigma_h$ that is equilibrated in the sense

$$\langle \operatorname{div}(\sigma_h), I_{\boldsymbol{V}_h} \boldsymbol{V}_0 \rangle_{\boldsymbol{V}_h} = (-\boldsymbol{f}, I_{\boldsymbol{V}_h} \boldsymbol{V}_0)$$

it holds

$$\|\nabla(\boldsymbol{u} - \bar{\mathbf{u}}_h)\|^2 \leqslant \eta(\sigma_h)^2 := \nu^{-2} \sum_{T \in \mathcal{T}} \Big(c_1 c_2 h_T^2 \|(\mathbf{id} - \boldsymbol{\pi}_{k-2}) \operatorname{curl}(\boldsymbol{f} + \operatorname{div}(\sigma_h))\|_T + \|\operatorname{dev}(\sigma_h - \bar{\sigma}_h)\|_T \Big)^2 + c_0^{-2} \|\operatorname{div} \bar{\mathbf{u}}_h\|^2.$$

Proof. As in Theorem 4.1 the point of departure is the error split

$$\|\nabla(\boldsymbol{u} - \bar{\mathbf{u}}_h)\|^2 \leqslant \nu^{-2} \|\boldsymbol{r}\|_{\boldsymbol{V}_0^\star}^2 + c_0^{-2} \|\operatorname{div} \bar{\mathbf{u}}_h\|^2$$

where it remains to bound the residual functional

$$\boldsymbol{r}(\boldsymbol{v}) = \int_\Omega \boldsymbol{f} \cdot \boldsymbol{v} \,\mathrm{d}x - \nu \int_\Omega \nabla \bar{\mathbf{u}}_h : \nabla \boldsymbol{v} \,\mathrm{d}x \quad \text{for all } \boldsymbol{v} \in \boldsymbol{V}_0$$

in its dual norm

$$\|\boldsymbol{r}\|_{\boldsymbol{V}_0^\star} := \sup_{\boldsymbol{v} \in \boldsymbol{V}_0 \setminus \{0\}} \frac{\boldsymbol{r}(\boldsymbol{v})}{\|\nabla \boldsymbol{v}\|}.$$

Consider an arbitrary test function $\boldsymbol{v} \in \boldsymbol{V}_0$ and some equilibrated flux σ_h with the properties stated above. Then, the insertion of $I_{\boldsymbol{V}_h} \boldsymbol{v}$ by the equilibration condition and an integration by parts show

$$\begin{aligned}\boldsymbol{r}(\boldsymbol{v}) &= \langle \boldsymbol{f} + \operatorname{div}(\sigma_h), \boldsymbol{v} - I_{\boldsymbol{V}_h} \boldsymbol{v} \rangle_{\boldsymbol{V}_h} + \int_\Omega (\sigma_h - \bar{\sigma}_h) : \nabla \boldsymbol{v} \,\mathrm{d}x \\ &= \sum_{T \in \mathcal{T}} \int_T (\boldsymbol{f} + \operatorname{div}(\sigma_h)) \cdot (\boldsymbol{v} - I_{\boldsymbol{V}_h} \boldsymbol{v}) \,\mathrm{d}x + \sum_{F \in \mathcal{F}(\Omega)} \int_F [\![(\sigma_h)_{nn}]\!] (\boldsymbol{v} - I_{\boldsymbol{V}_h} \boldsymbol{v}) \cdot \boldsymbol{n} \,\mathrm{d}s \\ &\quad + \int_\Omega (\sigma_h - \bar{\sigma}_h) : \nabla \boldsymbol{v} \,\mathrm{d}x.\end{aligned}$$

Since $[\![(\sigma_h)_{nn}]\!] \in P_k(F)$, the second integral vanishes due to orthogonality properties of the normal flux of $(\boldsymbol{v} - I_{\boldsymbol{V}_h} \boldsymbol{v})$. The last integral on the right-hand side can be estimated by

$$\int_\Omega (\sigma_h - \bar{\sigma}_h) : \nabla \boldsymbol{v} \,\mathrm{d}x = \int_\Omega \operatorname{dev}(\sigma_h - \bar{\sigma}_h) : \nabla \boldsymbol{v} \,\mathrm{d}x \leqslant \sum_{T \in \mathcal{T}} \|\operatorname{dev}(\sigma_h - \bar{\sigma}_h)\|_T \|\nabla \boldsymbol{v}\|_T. \tag{4.11}$$

Here, $\operatorname{dev}(A)$ denotes the deviatoric part of a A and it was used that $A - \operatorname{dev}(A) = \operatorname{tr}(A) I_{2\times 2}/2$ is orthogonal on gradients of divergence-free functions.

The first integral can be estimated as follows in $d = 3$ dimensions (for $d = 2$ the arguments are very similar). Since $\boldsymbol{v} - I_{\boldsymbol{V}_h}\boldsymbol{v}$ is divergence-free, it exists some $\boldsymbol{\psi} \in \boldsymbol{H}^1(\Omega)$ with $\|\nabla\boldsymbol{\psi}\|_T \leqslant \|\boldsymbol{v} - I_{\boldsymbol{V}_h}\boldsymbol{v}\|_T$, see for example in [8], such that $\boldsymbol{v} - I_{\boldsymbol{V}_h}\boldsymbol{v} = \operatorname{curl}\psi$ and by the interpolation properties we have

$$\|\nabla\boldsymbol{\psi}\|_T \leqslant \|\operatorname{curl}\boldsymbol{\psi}\|_T = \|\boldsymbol{v} - I_{\boldsymbol{V}_h}\boldsymbol{v}\|_T \leqslant c_1 h_T \|\nabla\boldsymbol{v}\|_T \quad \text{on every } T \in \mathcal{T}. \tag{4.12}$$

By the interpolation properties of $I_{\boldsymbol{V}_h}$, it holds $I_{\boldsymbol{V}_h}\operatorname{curl}\psi = 0$ and hence, by the commuting property (4.5) in Theorem 4.4, we also have that $\operatorname{curl} I_{W_h^3}\psi = 0$ where $I_{W_h^3}$ is the matching commuting interpolation operator. Note, that the application of the operator $I_{W_h^3}$ to $\boldsymbol{\psi}$ is well defined, since locally on each element $T \in \mathcal{T}$ we have that $\boldsymbol{v} - I_{\boldsymbol{V}_h}\boldsymbol{v} \in \boldsymbol{H}^1(T)$ and thus we can bound $\|\nabla\operatorname{curl}\boldsymbol{\psi}\|_T \leqslant \|\nabla(\boldsymbol{v} - I_{\boldsymbol{V}_h}\boldsymbol{v})\|_T$ which gives $\boldsymbol{\psi} \in \boldsymbol{H}^1(\operatorname{curl}, T)$.

Next, if $k \geqslant 2$, consider some Nedelec function $\boldsymbol{\theta}_h \in \mathcal{N}_{k-2}(\mathcal{T})$ chosen such that $\operatorname{curl}\boldsymbol{\theta}_h = \boldsymbol{\pi}_{k-2}\operatorname{curl}(\boldsymbol{f} + \operatorname{div}(\sigma_h))$ for which we can apply (4.9).

This, and the other properties of σ_h yield

$$\begin{aligned}\sum_{T\in\mathcal{T}}\int_T (\boldsymbol{f} + \operatorname{div}(\sigma_h))\cdot(\boldsymbol{v} - I_{\boldsymbol{V}_h}\boldsymbol{v})\,\mathrm{d}x &= \sum_{T\in\mathcal{T}}\int_T (\boldsymbol{f} + \operatorname{div}(\sigma_h) - \boldsymbol{\theta}_h)\cdot\operatorname{curl}(\boldsymbol{\psi} - I_{W_h^3}\boldsymbol{\psi})\,\mathrm{d}x\\ &= \sum_{T\in\mathcal{T}}\int_T (\mathbf{id} - \boldsymbol{\pi}_{k-2})\operatorname{curl}(\boldsymbol{f} + \operatorname{div}(\sigma_h))\cdot(\boldsymbol{\psi} - I_{W_h^3}\boldsymbol{\psi})\,\mathrm{d}x\\ &\quad + \sum_{F\in\mathcal{F}(\Omega)}\int_F [\![\boldsymbol{f} + \operatorname{div}(\sigma_h)]\!]\times\vec{n}\cdot(\boldsymbol{\psi} - I_{W_h^3}\boldsymbol{\psi})\,\mathrm{d}s.\end{aligned}$$

Since $\boldsymbol{f} \in H(\operatorname{curl}, \Omega)$ and $\operatorname{div}(\sigma_h) \in \boldsymbol{P}_{k-1}(\mathcal{T})$, the second integral vanishes due to properties (4.6) of $I_{W_h^3}$ from Theorem 4.4. For the remaining terms, the interpolation properties of $I_{W_h^3}$ (see again Theorem 4.4) and (4.12) yield

$$\begin{aligned}&\sum_{T\in\mathcal{T}}\int_T (\mathbf{id} - \boldsymbol{\pi}_{k-2})\operatorname{curl}(\boldsymbol{f} + \operatorname{div}(\sigma_h))\cdot(\psi - I_{W_h^3}\psi)\,\mathrm{d}x\\ &\qquad\leqslant \sum_{T\in\mathcal{T}}\|(\mathbf{id} - \boldsymbol{\pi}_{k-2})\operatorname{curl}(\boldsymbol{f} + \operatorname{div}(\sigma_h))\|_T\|\psi - I_{W_h^3}\psi\|_T\\ &\qquad\leqslant \sum_{T\in\mathcal{T}} c_2 h_T\|(\mathbf{id} - \boldsymbol{\pi}_{k-2})\operatorname{curl}(\boldsymbol{f} + \operatorname{div}(\sigma_h))\|_T\|\nabla\psi\|_T\\ &\qquad\leqslant \sum_{T\in\mathcal{T}} c_1 c_2 h_T^2\|(\mathbf{id} - \boldsymbol{\pi}_{k-2})\operatorname{curl}(\boldsymbol{f} + \operatorname{div}(\sigma_h))\|_T\|\nabla\boldsymbol{v}\|_T.\end{aligned}$$

The combination of the last estimate and (4.11) together with a Cauchy inequality yields

$$\boldsymbol{r}(\boldsymbol{v}) \leqslant \sum_{T\in\mathcal{T}}\left(c_1 c_2 h_T^2\|(\mathbf{id} - \boldsymbol{\pi}_{k-2})\operatorname{curl}(\boldsymbol{f} + \operatorname{div}(\sigma_h))\|_T + \|\operatorname{dev}(\sigma_h - \bar{\sigma}_h)\|_T\right)\|\nabla\boldsymbol{v}\|_T$$

and hence

$$\|\boldsymbol{r}\|_{\boldsymbol{V}_0^\star}^2 \leqslant \sum_{T\in\mathcal{T}}\left(c_1 c_2 h_T^2\|(\mathbf{id} - \boldsymbol{\pi}_{k-2})\operatorname{curl}(\boldsymbol{f} + \operatorname{div}(\sigma_h))\|_T + \|\operatorname{dev}(\sigma_h - \bar{\sigma}_h)\|_T\right)^2,$$

what concludes the proof. □

Remark 4.6. Theorem 4.5 also holds true in the case when we only have the local regularity assumption $\boldsymbol{f} \in H(\operatorname{curl}, T)$ for all $T \in \mathcal{T}$. Note however, that this introduces another term on the boundary of the elements given by

$$c_3\sum_{F\in\mathcal{F}(\Omega)} h_F^3\|(\mathbf{id} - \boldsymbol{\pi}_{k-1})[\![\boldsymbol{f}\times\boldsymbol{n}]\!]\|_F^2$$

added to the estimator $\eta(\sigma_h)^2$ given in Theorem 4.5. Here, c_3 is an additional constant that only depends on the shape of the simplicies $T \in \mathcal{T}$.

Remark 4.7 (Global MCS estimator)**.** One possible choice is $\sigma_h = \sigma_h^{\mathrm{MCS}}$, where σ_h^{MCS} is the solution of the global mass conserving mixed stress formulation (3.6) of order k. Another choice can be achieved by a local strategy that is detailed in the next section.

Remark 4.8 (Divergence quantity)**.** In the numerical examples below, it becomes apparent that the efficiency of the error estimator is mostly limited by the divergence-term $c_0^{-1}\|\operatorname{div} \boldsymbol{u}_h\|$ for non-divergence-free discretisations. To avoid this term and possibly further increase the efficiency, one may consider a divergence-free postprocessing $\boldsymbol{s}_h \in \boldsymbol{H}^1(\Omega)$ of $\boldsymbol{u}_h$ and perform the error estimation for $\boldsymbol{s}_h$ or $\bar{\sigma}_h := \nabla \boldsymbol{s}_h$. Effectively this would replace the term $c_0^{-1}\|\operatorname{div} \boldsymbol{u}_h\|$ by $\|\nabla(\boldsymbol{s}_h - \bar{\boldsymbol{u}}_h)\|$ without the possibly small constant c_0. Candidates for such a postprocessing maybe a locally computed approximation into a divergence-free Scott-Vogelius finite element space (on a barycentrically refined subgrid) similar to [20].

5. Local Equilibration

This section suggests some design of an admissible pressure-robust equilibrated flux σ_h based on local problems on vertex patches.

5.1. **Setup of the local problems.** Let $\mathcal{V}$ be the set of vertices for $V \in \mathcal{V}$ let ω_V be the corresponding vertex patch, i.e. the union of all adjacent cells in $\mathcal{T}_V := \{T \in \mathcal{T} : V \in \overline{T}\}$. Furthermore, $\mathcal{F}_V$ denotes the set of facets within the vertex patch including the facets on the boundary $\partial\omega_V$. For a fixed interior vertex V we define the following spaces with $k = r$ (recall that r is the optimal convergence rate of the primal method)

$$\begin{aligned}
\Sigma_h^V &:= \{\tau_h \in L^2(\mathcal{T}_V)^{d\times d} : \forall T \in \mathcal{T}_V,\ \tau_h|_T \in P_k(T)^{d\times d} \text{ with } \operatorname{tr}(\tau_h) = 0\},\\
\tilde{\boldsymbol{V}}_h^V &:= \mathrm{RT}_k(\mathcal{T}_V),\\
\hat{\boldsymbol{V}}_h^V &:= \{\hat{\boldsymbol{v}}_h \in \boldsymbol{L}^2(\mathcal{F}_V) : \forall F \in \mathcal{F}_V,\ \hat{\boldsymbol{v}}_h|_F \in \boldsymbol{P}_k(F) \text{ and } \hat{\boldsymbol{v}}_h \cdot n = 0\},\\
Q_h^V &:= \{q_h \in L^2(\omega_V) : \forall T \in \mathcal{T}_V,\ q_h|_T \in P_k(T)\}.
\end{aligned}$$

Note, that in contrast to the global stress space Σ_h, the local stress space Σ_h^V does not include the continuity constraint $[\![(\tau_h)_{nt}]\!] = 0$. Similarly to other local equilibration setups, see for example [4], the trace space V_h^V is chosen such that the normal-tangential trace of functions in Σ_h^V lie in V_h^V. For the local problems we then further define the product space

$$\boldsymbol{V}_h^V := (\tilde{\boldsymbol{V}}_h^V \times \hat{\boldsymbol{V}}_h^V)/\{((c_1,c_2),(c_1,c_2)_t) : (c_1,c_2) \in \mathbb{R}^2\}, \tag{5.1}$$

where (c_1,c_2) denotes a vector valued constant, and $((c_1,c_2),(c_1,c_2)_t)$ reads as (a constant) element of the product space $\tilde{\boldsymbol{V}}_h^V \times \hat{\boldsymbol{V}}_h^V$. Hence, the space $\boldsymbol{V}_h^V$ does not contain vector-valued constant functions on the patch. The projection onto constants $\boldsymbol{\pi}_{\mathbb{R}}^V : L^2(\mathcal{T}_V)^2 \times [L^2(\mathcal{F}_V)^2]_t \to (\mathbb{R},\mathbb{R})$ is given by

$$\boldsymbol{\pi}_{\mathbb{R}}^V(\tilde{\boldsymbol{v}}_h,\hat{\boldsymbol{v}}_h) := \frac{1}{|\mathcal{T}_V| + |\mathcal{F}_V|}\left(\sum_{T\in\mathcal{T}_V}\int_T \tilde{\boldsymbol{v}}_h \,\mathrm{d}x + \sum_{F\in\mathcal{F}_V}\int_F \hat{\boldsymbol{v}}_h \,\mathrm{d}s\right).$$

Here, $|\mathcal{T}_V|$ and $|\mathcal{F}_V|$ denote the area of the element patch and the skeleton of the patch respectively. Note, that we then have the equality

$$\boldsymbol{V}_h^V = \{(\tilde{\boldsymbol{v}}_h,\hat{\boldsymbol{v}}_h) \in \tilde{\boldsymbol{V}}_h^V \times \hat{\boldsymbol{V}}_h^V : (\mathbf{id} - \boldsymbol{\pi}_{\mathbb{R}}^V)(\tilde{\boldsymbol{v}}_h,\hat{\boldsymbol{v}}_h) \neq (0,0)\}. \tag{5.2}$$

For each element T and every vertex $V \in T$ we define the scalar linear operator

$$B_T^V : P_{k+1}(T) \to P_{k+1}(T),\ q \mapsto B_T^V(q) := I_{\mathcal{N}}^{k+1}(\phi_V q),$$

where $I_{\mathcal{N}}^{k+1}$ is the nodal interpolation operator on $P_{k+1}(T)$ and ϕ_V is the hat function of the vertex V. By that we then define on ω_V the scalar bubble projector (see also [21])

$$B^V : P_{k+1}(\mathcal{T}_V) \to P_{k+1}(\mathcal{T}_V),\ q \mapsto B^V(q) := \sum_{T\in\mathcal{T}_V} B_T^V(q),$$

and the vector valued bubble projector

$$\boldsymbol{B}^V : \boldsymbol{P}_{k+1}(\mathcal{T}_V) \to \boldsymbol{P}_{k+1}(\mathcal{T}_V),\ \boldsymbol{q} = (q_1, q_2) \mapsto \boldsymbol{B}^V(\boldsymbol{q}) := (B^V(q_1), B^V(q_2)).$$

Lemma 5.1. The vector valued bubble projector $\boldsymbol{B}^V$ fulfills the following properties:

i. $\boldsymbol{B}^V(\boldsymbol{q})|_{\partial\omega_V} = 0$ for all $\boldsymbol{q} \in \boldsymbol{P}_k(\mathcal{T}_V)$.
ii. $\boldsymbol{B}^V(\tilde{\boldsymbol{v}}_h^V) \in \tilde{\boldsymbol{V}}_h^V$ for all $\tilde{\boldsymbol{v}}_h^V \in \tilde{\boldsymbol{V}}_h^V$. Further, if $\operatorname{div}(\tilde{\boldsymbol{v}}_h^V) = 0$, then $\boldsymbol{B}^V(\tilde{\boldsymbol{v}}_h^V) \in \mathrm{BDM}_k(\mathcal{T}_V)$.
iii. For all elements $T \in \mathcal{T}$ we have the partition of unity property

$$\sum_{V\in T} \boldsymbol{B}^V(\boldsymbol{v}_h|_T) = \boldsymbol{v}_h|_T \quad \text{for all } \boldsymbol{v}_h \in \boldsymbol{V}_h.$$

iv. For a constant $c = (c_1, c_2) \in \boldsymbol{P}_0(\omega_V)$ there holds $\boldsymbol{B}^V(c) = \phi_V(c_1, c_2)$.

Proof. Items *i.* and *iii.* follow by the definition and the linearity of the bubble projection. For the proof of *ii.* choose an arbitrary edge $F \in \mathcal{F}_V$ with the corresponding normal vector $\boldsymbol{n}$. Since $\tilde{\boldsymbol{v}}_h^V$ is normal continuous we have by the properties of the nodal interpolation operator

$$[\![\boldsymbol{B}^V(\tilde{\boldsymbol{v}}_h^V)(x_i)\cdot\boldsymbol{n}]\!] = \phi_V(x_i)[\![\tilde{\boldsymbol{v}}_h^V(x_i)\cdot n]\!] = 0 \quad \text{for all } x_i \in F.$$

The second statment immediately follows since if $\tilde{\boldsymbol{v}}_h^V \in \tilde{\boldsymbol{V}}_h^V = \mathrm{RT}^k(\mathcal{T}_V)$ is divergence-free, then $\tilde{\boldsymbol{v}}_h^V \in \mathrm{BDM}^k(\mathcal{T}_V)$. For *iv.* note that for $j = 1, 2$ there holds on each element $T \in \mathcal{T}_V$ that $I_{\mathcal{N}}^{k+1}(c_j\phi_V) = c_j\phi_V$ hence we conclude the proof. □

For each vertex V we solve the local problem: Find $(\sigma_h^V, (\tilde{\boldsymbol{u}}_h^V, \hat{\boldsymbol{u}}_h^V), p_h^V) \in \Sigma_h^V \times \boldsymbol{V}_h^V \times Q_h^V$ such that

(5.3a) $$a^V(\sigma_h^V, \tau_h^V) + b_1^V(\tau_h^V, (\tilde{\boldsymbol{u}}_h^V, \hat{\boldsymbol{u}}_h^V)) = 0 \qquad \text{for all } \tau_h^V \in \Sigma_h^V,$$

(5.3b) $$b_1^V(\sigma_h^V, (\tilde{\boldsymbol{v}}_h^V, \hat{\boldsymbol{v}}_h^V)) + b_2(\tilde{\boldsymbol{v}}_h^V, p_h^V) = G_1^V(\boldsymbol{f}, \bar{\boldsymbol{u}}_h, \bar{p}_h)((\tilde{\boldsymbol{v}}_h^V, \hat{\boldsymbol{v}}_h^V)) \qquad \text{for all } (\tilde{\boldsymbol{v}}_h^V, \hat{\boldsymbol{v}}_h^V) \in \boldsymbol{V}_h^V,$$

(5.3c) $$b_2^V(\tilde{\boldsymbol{u}}_h^V, q_h^V) = 0 \qquad \text{for all } q_h^V \in q_h^V,$$

with the bilinearforms

$$a_h^V(\sigma_h^V, \tau_h^V) := \sum_{T\in\mathcal{T}_V} \int_K \sigma_h^V \cdot \tau_h^V \,\mathrm{d}x,$$

$$b_1^V(\tau_h^V, (\tilde{\boldsymbol{u}}_h^V, \hat{\boldsymbol{u}}_h^V)) := \sum_{T\in\mathcal{T}_V} \int_T \operatorname{div}(\tau_h^V)\cdot\tilde{\boldsymbol{u}}_h^V \,\mathrm{d}x - \sum_{F\in\mathcal{F}_V}\int_F ([\![(\tau_h^V)_{nn}]\!](\tilde{\boldsymbol{u}}_h^V)_n + [\![(\tau_h^V)_{nt}]\!]\cdot\hat{\boldsymbol{u}}_h^V)\,\mathrm{d}s,$$

$$b_2^V(\tilde{\boldsymbol{u}}_h^V, q_h^V) := \sum_{T\in\mathcal{T}_V} \int_T \operatorname{div}(\tilde{\boldsymbol{u}}_h^V) q_h^V \,\mathrm{d}x,$$

and the linear form (for a given $\boldsymbol{f}, \bar{\boldsymbol{u}}_h, \bar{p}_h$)

$$\begin{aligned} G_1^V(\boldsymbol{f}, \bar{\boldsymbol{u}}_h, \bar{p}_h)(\tilde{\boldsymbol{v}}_h^V, \hat{\boldsymbol{v}}_h^V) = &\sum_{T\in\mathcal{T}_V}\int_T \boldsymbol{f}\cdot\boldsymbol{B}^V(\tilde{\boldsymbol{v}}_h^V)\,\mathrm{d}x + \sum_{T\in\mathcal{T}_V}\int_T (\nu\Delta\bar{\boldsymbol{u}}_h - \nabla\bar{p}_h)\cdot\boldsymbol{B}^V(\tilde{\boldsymbol{v}}_h^V)\,\mathrm{d}x \\ &- \int_{\partial T}(\bar{\sigma}_h - \bar{p}_h I)_{nn}\boldsymbol{B}^V(\tilde{\boldsymbol{v}}_h^V)_n\,\mathrm{d}s - \int_{\partial T}\phi_V(\sigma_h)_{nt}(\hat{\boldsymbol{v}}_h^V)_t\,\mathrm{d}s. \end{aligned}$$

Note, that $b_1^V(\cdot,\cdot)$ reads as the restriction of the discrete duality pair $\langle\operatorname{div}(\cdot),\cdot\rangle_{\boldsymbol{V}_h}$ onto ω_V, but further includes the normal-tangential jumps since functions in Σ_h^V are not (normal-tangential) continuous. Using integration by

parts, the right hand side can also be written as

$$G_1^V(\tilde{\boldsymbol{v}}_h^V, \hat{\boldsymbol{v}}_h^V) = \sum_{T\in\mathcal{T}_V}\int_T \boldsymbol{f}\cdot\boldsymbol{B}^V(\tilde{\boldsymbol{v}}_h^V)\,\mathrm{d}x - \int_T \bar{\sigma}_h : \nabla\boldsymbol{B}^V(\tilde{\boldsymbol{v}}_h^V)\,\mathrm{d}x + \int_T \bar{p}_h\,\mathrm{div}(\boldsymbol{B}^V(\tilde{\boldsymbol{v}}_h^V))\,\mathrm{d}x + \int_{\partial T}(\bar{\sigma}_h)_{nt}(\boldsymbol{B}^V(\tilde{\boldsymbol{v}}_h^V) - \phi_V\hat{\boldsymbol{v}}_h^V)_t\,\mathrm{d}s. \tag{5.5}$$

Remark 5.2. For simplicity we used a muliplication with the hat function ϕ_V instead of the bubble projection in the last integral of G_1^V. Note however, that since $(\sigma_h)_{nt}\in\boldsymbol{P}^k(F)$ for all $F\in\mathcal{F}^V$, this is identical, i.e.

$$\int_{\partial T}\phi_V(\sigma_h)_{nt}(\hat{\boldsymbol{v}}_h^V)_t\,\mathrm{d}s = \int_{\partial T}\boldsymbol{B}^V|_F((\sigma_h)_{nt})(\hat{\boldsymbol{v}}_h^V)_t\,\mathrm{d}s,$$

where $\boldsymbol{B}^V|_F((\sigma_h)_{nt})$ reads as the nodal interpolation into the vector valued polynomial space of order $k+1$ on F of the quantity $(\sigma_h)_{nt}$.

Remark 5.3. As usual for equilibrated error estimators, we slightly modify the definition of the local problems when the vertex V lies on the Dirichlet boundary. In this case, we remove the degrees of freedoms of $\hat{\boldsymbol{V}}_h^V$ lying on the domain boundary. Hence, we now replace $\mathcal{F}_V$ by $\mathcal{F}_V\backslash\{F\in\mathcal{F}_V : F\subset\partial\Omega\}$. Further, we remove the mean value constraint of the product space, thus we simply set $\boldsymbol{V}_h^V := (\tilde{\boldsymbol{V}}_h^V\times\hat{\boldsymbol{V}}_h^V)$.

5.2. **Analysis of the local problem.** For the analysis we choose the norms

$$\|\sigma_h^V\|_{\Sigma_h^V}^2 := \sum_T \|\sigma_h^V\|_T^2 + h_T\|(\sigma_h^V)_{nt}\|_{\partial T}^2,$$
$$\|(\tilde{\boldsymbol{v}}_h^V,\hat{\boldsymbol{v}}_h^V)\|_{V_h^V}^2 := \sum_T \|\nabla\tilde{\boldsymbol{v}}_h^V\|_T^2 + \frac{1}{h_T}\|(\hat{\boldsymbol{v}}_h^V - \tilde{\boldsymbol{v}}_h^V)_t\|_{\partial T}^2,$$
$$\|p_h^V\|_{Q_h^V} = \|p_h^V\|.$$

Note, that the the norm $\|\cdot\|_{V_h^V}$ reads as an HDG-version of the H^1-like DG norm $\|\cdot\|_{V_h}$ defined in Section 3.3. Further we define the kernel

$$\mathcal{K}_1^V := \left\{(\sigma_h^V,p_h^V) : \forall(\tilde{\boldsymbol{v}}_h^V,\hat{\boldsymbol{v}}_h^V)\in\boldsymbol{V}_h^V,\ b_1^V(\sigma_h^V,(\tilde{\boldsymbol{v}}_h^V,\hat{\boldsymbol{v}}_h^V)) + b_2^V(\tilde{\boldsymbol{v}}_h^V,p_h^V) = 0\right\}.$$

Lemma 5.4. The bilinear forms a^V, b_1^V, b_2^V are continuous. Further there holds the kernel ellipticity

$$a^V(\sigma_h^V,\tau_h^V) \gtrsim (\|\sigma_h^V\|_{\Sigma_h^V}\|^2 + \|p_h^V\|_{Q_h^V}^2) \quad \text{for all } (\sigma_h^V,p_h^V)\in\mathcal{K}_1^V,$$

and the inf-sup conditions

1 For all $(\tilde{\boldsymbol{v}}_h^V,\hat{\boldsymbol{v}}_h^V)\in\boldsymbol{V}_h^V$ there exists a constant $\beta_1>0$ such that

$$\sup_{(\sigma_h^V,p_h^V)\in\Sigma_h^V\times Q_h^V}\frac{b_1^V(\sigma_h^V,(\tilde{\boldsymbol{v}}_h^V,\hat{\boldsymbol{v}}_h^V)) + b_2^V(\tilde{\boldsymbol{v}}_h^V,p_h^V)}{\|\sigma_h^V\|_{\Sigma_h^V}\| + \|p_h^V\|_{Q_h^V}} \geqslant \beta_1\|(\tilde{\boldsymbol{v}}_h^V,\hat{\boldsymbol{v}}_h^V)\|_{V_h^V}.$$

2 For all $(\tilde{\boldsymbol{v}}_h^V,\hat{\boldsymbol{v}}_h^V)\in\boldsymbol{V}_h^V$ with $\mathrm{div}(\tilde{\boldsymbol{v}}_h^V)=0$ there exists a constant $\beta_2>0$ such that

$$\sup_{\sigma_h^V\in\Sigma_h^V}\frac{b_1^V(\sigma_h^V,(\tilde{\boldsymbol{v}}_h^V,\hat{\boldsymbol{v}}_h^V))}{\|\sigma_h^V\|_{\Sigma_h^V}} \geqslant \beta_2\|(\tilde{\boldsymbol{v}}_h^V,\hat{\boldsymbol{v}}_h^V)\|_{V_h^V}.$$

Proof. The continuity of the bilinear forms follows immediately with the Cauchy-Schwarz inequality and using integration by parts for the volume integrals of b_1^V. The proofs of the kernel ellipticity and the inf-sup conditions follow with exactly the same steps as in the stability proofs of the original MCS-method in [15, 14, 22], since the bilinear forms and spaces of the local problems in this work simply read as a hybridized version of the original MCS-method. In this work the normal-tangential continuity of the stress space is incorporated by the additional Lagrange multiplier $\hat{\boldsymbol{u}}_h^V$ and we switched from the H^1-like DG norm used in the original works to the corresponding H^1-like HDG norm given by $\|\cdot\|_{V_h^V}$ in this work. Note however, that we do not have zero Dirichlet boundary conditions of

the velocity variable, but since we excluded the kernel of $\|\cdot\|_{V_h^V}$ (constant functions) in the definition of the space $\boldsymbol{V}_h^V$, the results simply follow by norm equivalence. □

Theorem 5.5. There exists an unique solution $(\sigma_h^V, (\tilde{\boldsymbol{u}}_h^V, \hat{\boldsymbol{u}}_h^V), p_h^V) \in \Sigma_h^V \times \boldsymbol{V}_h^V \times Q_h^V$ of (5.3) with the stability estimate

$$\|\sigma_h^V\|_{\Sigma_h^V} + \|(\tilde{\boldsymbol{u}}_h^V, \hat{\boldsymbol{u}}_h^V)\|_{V_h^V} + \|p_h^V\|_{Q_h^V} \lesssim \|G_1^V(\boldsymbol{f}, \bar{\boldsymbol{u}}_h, p_h)\|_{(\boldsymbol{V}_h^V)^\star}.$$

Proof. Follows with the standard theory of saddle point problems, see for example in [3] and Lemma 5.4. □

Now let $\hat{\boldsymbol{V}}_h$ be the global version of the local space $\hat{\boldsymbol{V}}_h^V$, thus

$$\hat{\boldsymbol{V}}_h := := \{\hat{\boldsymbol{v}}_h \in \boldsymbol{L}^2(\mathcal{F}) : \forall F \in \mathcal{F},\ \hat{\boldsymbol{v}}_h|_F \in \boldsymbol{P}_k(F) \text{ and } \hat{\boldsymbol{v}}_h \cdot \boldsymbol{n} = 0\}.$$

Theorem 5.6 (Properties of the local solution)**.** Let $\sigma_h^V \in \Sigma_h^V$ be the local solution of problem (5.3). There holds the following properties:

1 For any $\boldsymbol{v}_h \in \boldsymbol{V}_h$, with $\operatorname{div} \boldsymbol{v}_h = 0$, and $\hat{\boldsymbol{v}}_h \in \hat{\boldsymbol{V}}_h$, there holds the local equilibrium condition

$$\begin{aligned}
&\sum_{T\in\mathcal{T}_V} \int_T \operatorname{div}(\sigma_h^V) \cdot \boldsymbol{v}_h - \sum_{F\in\mathcal{F}_V} \int_F [\![(\sigma_h^V)_{nn}]\!](\boldsymbol{v}_h)_n - \sum_F \int_{F\in\mathcal{F}_V} [\![(\sigma_h^V)_{nt}]\!] \cdot (\hat{\boldsymbol{v}}_h)_t \\
&= \sum_{T\in\mathcal{T}_V} \int_T \boldsymbol{f} \cdot \boldsymbol{B}^V(\boldsymbol{v}_h)\,\mathrm{d}x - \int_T \bar{\sigma}_h : \nabla \boldsymbol{B}^V(\boldsymbol{v}_h)\,\mathrm{d}x + \int_T \phi_V \bar{p}_h \operatorname{div}(\boldsymbol{B}^V(\boldsymbol{v}_h))\,\mathrm{d}x \\
&+ \int_{\partial T} (\bar{\sigma}_h)_{nt} \cdot (\boldsymbol{B}^V(\boldsymbol{v}_h) - \phi_V \hat{\boldsymbol{v}}_h)_t\,\mathrm{d}s.
\end{aligned}$$

2 The solution σ_h has a zero normal-tangential trace at the boundary

$$(\sigma_h^V)_{nt} = 0 \quad \text{on} \quad \partial\omega_V.$$

Proof. Let $V \in \mathcal{V}$ be fixed and let $\tilde{\boldsymbol{v}}_h^V = \boldsymbol{v}_h|_{\omega_V}$ and $\hat{\boldsymbol{v}}_h^V = \hat{\boldsymbol{v}}_h|_{\mathcal{F}_V}$. In a first step we will proof that equation (5.3b) also hold for constant functions. To this end let $c = (c_1, c_2) = \boldsymbol{\pi}_{\mathbb{R}}^V((\tilde{\boldsymbol{v}}_h^V, \hat{\boldsymbol{v}}_h^V))$. Using $\operatorname{div}(c) = 0$ and integration by parts we have for the left side of (5.3b)

$$\begin{aligned}
&b_1^V(\sigma_h^V, (c, c_t)) + b_2(c, p_h^V) \\
&\qquad = \sum_T \int_T \operatorname{div}(\sigma_h^V) \cdot (c_1, c_2)\,\mathrm{d}x - \sum_F \int_F ([\![(\sigma_h^V)_{nn}]\!](c_1, c_2)_n + [\![(\sigma_h^V)_{nt}]\!] \cdot (c_1, c_2)_t)\,\mathrm{d}s \\
&\qquad = -\sum_T \int_T \sigma_h^V : \nabla(c_1, c_2) + \sum_F \int_F [\![(\sigma_h^V)_{nt}]\!] \cdot ((c_1, c_2) - (c_1, c_2))_t = 0.
\end{aligned}$$

We continue with the right-hand side. Using representation (5.5) we get for the constant c and using property *iv.* of Lemma 5.1 that

$$\begin{aligned}
&G_1^V((c_1, c_2), (c_1, c_2)_t) \\
&= \sum_{T\in\mathcal{T}_V} \int_T \boldsymbol{f} \cdot \boldsymbol{B}^V((c_1, c_2))\,\mathrm{d}x - \int_T \bar{\sigma}_h : \nabla \boldsymbol{B}^V((c_1, c_2))\,\mathrm{d}x + \int_T \phi_V \bar{p}_h \operatorname{div}(\boldsymbol{B}^V((c_1, c_2)))\,\mathrm{d}x \\
&\quad + \int_{\partial T} (\bar{\sigma}_h)_{nt} \cdot (\boldsymbol{B}^V((c_1, c_2))_t - \phi_V (c_1, c_2)_t)\,\mathrm{d}s \\
&= \sum_{T\in\mathcal{T}_V} \int_T \boldsymbol{f} \cdot (c_1\phi_V, c_2\phi_V)\,\mathrm{d}x - \int_T \bar{\sigma}_h : \begin{pmatrix} \nabla(c_1\phi_V) \\ \nabla(c_2\phi_V) \end{pmatrix} \mathrm{d}x + \int_T \bar{p}_h \operatorname{div}(c\phi_V)\,\mathrm{d}x.
\end{aligned}$$

Now, since $(c\phi_V, c\phi_V)$ is an element of the velocity Stokes discretization space $\bar{\boldsymbol{V}}_h$ (see assumption above equation (3.5)), and $\bar{\sigma}_h = \nabla \bar{\boldsymbol{u}}_h$ we also get

$$G_1^V((c_1,c_2),(c_1,c_2)_t) = \sum_{T\in\mathcal{T}_V} \int_T \boldsymbol{f}\cdot(\mathbf{id}-\mathcal{R})(c\phi_V, c\phi_V) = 0,$$

where the last equality follows since $(c\phi_V, c\phi_V) \in \boldsymbol{P}_{1,c}$ and (3.5). In total, this shows that we also have $G_1^V((c_1,c_2)) = 0$, thus using $(\tilde{\boldsymbol{v}}_h^V, \hat{\boldsymbol{v}}_h^V) = (\boldsymbol{\pi}_{\mathbb{R}}^V + (id - \boldsymbol{\pi}_{\mathbb{R}}^V))(\tilde{\boldsymbol{v}}_h^V, \hat{\boldsymbol{v}}_h^V)$ and the equivalence (5.2) we get

$$b_1^V(\sigma_h^V, (\tilde{\boldsymbol{v}}_h^V, \hat{\boldsymbol{v}}_h^V)) + b_2(\tilde{\boldsymbol{v}}_h^V, p_h^V) = G_1^V(\boldsymbol{f}, \bar{\boldsymbol{u}}_h, \bar{p}_h)((\tilde{\boldsymbol{v}}_h^V, \hat{\boldsymbol{v}}_h^V)) \quad \text{for all } (\tilde{\boldsymbol{v}}_h^V, \hat{\boldsymbol{v}}_h^V) \in \tilde{\boldsymbol{V}}_h^V \times \hat{\boldsymbol{V}}_h^V. \tag{5.6}$$

Since $\operatorname{div}(\boldsymbol{v}_h) = 0$ and thus $b_2(\tilde{\boldsymbol{v}}_h^V, p_h^V) = 0$, this proofs the first statement.

For the proof of the second statement consider the testfunction $\hat{\boldsymbol{v}}_h^V \in \hat{\boldsymbol{V}}_h^V$ such that $\hat{\boldsymbol{v}}_h^V = (\sigma_h^V)_{nt}$ on every facet $F \subset \partial\omega_V$, and zero on the internal facets. Equation (5.6) then gives

$$-\sum_{F\in\partial\omega_V}\int_F (\sigma_h^V)_{nt}^2\,\mathrm{d}s = -\sum_{F\in\partial\omega_V}\int_F (\sigma_h^V)_{nt}\cdot\hat{\boldsymbol{v}}_h^V\,\mathrm{d}s = -\sum_{T\in\mathcal{T}_V}\int_{\partial T}\phi_V(\bar{\sigma}_h)_{nt}\cdot\hat{\boldsymbol{v}}_h^V\,\mathrm{d}s = 0,$$

where we used that ϕ_V vanishes on the boundary $\partial\omega_V$ and $\hat{v}_h^V$ on internal facets. □

5.3. **Admissibility of the global flux.** After solving the local problems we define the equilibrated flux

$$\sigma_h^{\mathsf{LEQ}} := \bar{\sigma}_h - \sigma_h^{\Delta} \quad \text{with} \quad \sigma_h^{\Delta} := \sum_V \sigma_h^V. \tag{5.7}$$

This section shows that σ_h^{LEQ} satisfies the global equilibration property of Theorem 4.5.

Theorem 5.7. Let $\boldsymbol{v}_h \in \mathrm{RT}_k(\mathcal{T})$, with $\operatorname{div}(\boldsymbol{v}_h) = 0$. There holds

$$\sum_{T\in\mathcal{T}}\int_T \operatorname{div}(\sigma_h^{\mathsf{LEQ}})\cdot\boldsymbol{v}_h\,\mathrm{d}x - \sum_{F\in\mathcal{F}}\int_F [\![(\sigma_h^{\mathsf{LEQ}})_{nn}]\!](\boldsymbol{v}_h)_n\,\mathrm{d}s = -\int_\Omega \boldsymbol{f}\cdot\boldsymbol{v}_h\,\mathrm{d}x = -\int_\Omega \mathbb{P}(\boldsymbol{f})\cdot\boldsymbol{v}_h\,\mathrm{d}x.$$

Proof. In a first step we show that $\sigma_h^{\mathsf{LEQ}} \in \Sigma_h(\mathcal{T})$. For this let $\hat{\boldsymbol{v}}_h \in \hat{V}_h$ be arbitrary, then there holds

$$\begin{aligned}
\sum_{F\in\mathcal{F}}\int_F [\![(\sigma_h^{\mathsf{LEQ}})_{nt}]\!]\cdot(\hat{\boldsymbol{v}}_h)_t\,\mathrm{d}s &= \sum_{F\in\mathcal{F}}\sum_{V\in\partial F}\int_F [\![(\sigma_h^{\mathsf{LEQ}})_{nt}]\!]\cdot(\phi_V\hat{\boldsymbol{v}})_t\,\mathrm{d}s \\
&= \sum_{V\in\mathcal{V}}\sum_{F\in\mathcal{F}_V}\int_F [\![(\sigma_h^{\mathsf{LEQ}})_{nt}]\!]\cdot(\phi_V\hat{\boldsymbol{v}}_h)_t\,\mathrm{d}s \\
&= \sum_{V\in\mathcal{V}}\sum_{F\in\mathcal{F}_V}\int_F [\![(\bar{\sigma}_h)_{nt}]\!]\cdot(\phi_V\hat{\boldsymbol{v}}_h)_t\,\mathrm{d}s - \int_F [\![(\sigma_h^{\Delta})_{nt}]\!]\cdot(\phi_V\hat{\boldsymbol{v}}_h)_t\,\mathrm{d}s,
\end{aligned}$$

where we used a partition of unity on each $F \in \mathcal{F}$ in the first step. Applying the second and then the first statement of Theorem 5.6 (with $\boldsymbol{v}_h = 0$), the sum over the last integral can be written as

$$\begin{aligned}
-\sum_{V\in\mathcal{V}}\sum_{F\in\mathcal{F}_V}\int_F [\![(\sigma_h^{\Delta})_{nt}]\!]\cdot(\phi_V\hat{\boldsymbol{v}}_h)_t\,\mathrm{d}s &= -\sum_{V\in\mathcal{V}}\sum_{F\in\mathcal{F}_V}\int_F [\![(\sigma_h^{V})_{nt}]\!]\cdot(\phi_V\hat{\boldsymbol{v}}_h)_t\,\mathrm{d}s \\
&= -\sum_{V\in\mathcal{V}}\sum_{F\in\mathcal{F}_V}\int_F [\![(\bar{\sigma}_h)_{nt}]\!]\cdot(\phi_V\hat{\boldsymbol{v}}_h)_t\,\mathrm{d}s,
\end{aligned}$$

and thus

$$\sum_{F\in\mathcal{F}}\int_F [\![(\sigma_h^{\mathsf{LEQ}})_{nt}]\!]\cdot(\hat{\boldsymbol{v}}_h)_t\,\mathrm{d}s = 0. \tag{5.8}$$

With the choice $\hat{\boldsymbol{v}}_h = [\![(\sigma_h^{\mathsf{LEQ}})_{nt}]\!]$, we conclude that $[\![(\sigma_h^{\mathsf{LEQ}})_{nt}]\!] = 0$ point wise, and so $\sigma_h^{\mathsf{LEQ}} \in \Sigma_h(\mathcal{T})$.

Now let $\boldsymbol{v}_h \in V_h$ with $\operatorname{div}(\boldsymbol{v}_h) = 0$, and $\hat{\boldsymbol{v}}_h \in \hat{\boldsymbol{V}}_h$ be arbitrary. Using equation (5.8), the definition of σ_h^{LEQ} and integration by parts give

$$\begin{aligned}
&\sum_{T\in\mathcal{T}}\int_T \operatorname{div}(\sigma_h^{\mathsf{LEQ}})\cdot\boldsymbol{v}_h\,\mathrm{d}x - \sum_{F\in\mathcal{F}}\int_F [\![(\sigma_h^{\mathsf{LEQ}})_{nn}]\!](\boldsymbol{v}_h)_n\,\mathrm{d}s\\
&= \sum_{T\in\mathcal{T}}\int_T \operatorname{div}(\sigma_h^{\mathsf{LEQ}})\cdot\boldsymbol{v}_h\,\mathrm{d}x - \sum_{F\in\mathcal{F}}\int_F [\![(\sigma_h^{\mathsf{LEQ}})_{nn}]\!](\boldsymbol{v}_h)_n\,\mathrm{d}s - \sum_{F\in\mathcal{F}}\int_F [\![(\sigma_h^{\mathsf{LEQ}})_{nt}]\!]\cdot(\hat{\boldsymbol{v}}_h)_t\,\mathrm{d}s\\
&= \sum_{T\in\mathcal{T}}\int_T -\bar{\sigma}_h : \nabla\boldsymbol{v}_h\,\mathrm{d}x + \int_{\partial T}(\bar{\sigma}_h)_{nt}\cdot(\boldsymbol{v}_h-\hat{\boldsymbol{v}}_h)_t\,\mathrm{d}s + \sum_{T\in\mathcal{T}}\int_T \sigma_h^{\Delta} : \nabla\boldsymbol{v}_h\,\mathrm{d}x\\
&\qquad - \int_{\partial T}(\sigma_h^{\Delta})_{nt}\cdot(\boldsymbol{v}_h-\hat{\boldsymbol{v}}_h)_t\,\mathrm{d}s.
\end{aligned}$$

Since $\sigma_h^{\Delta} := \sum_V \sigma_h^V$, a partition of unity and the local contributions σ_h^V let us rewrite the last sums as

$$\begin{aligned}
\sum_{T\in\mathcal{T}}\int_T \sigma_h^{\Delta} : \nabla\boldsymbol{v}_h\,\mathrm{d}x - \int_{\partial T}(\sigma_h^{\Delta})_{nt}\cdot(\boldsymbol{v}_h-\hat{\boldsymbol{v}}_h)_t\,\mathrm{d}s &= \sum_{V\in\mathcal{V}}\sum_{T\in\mathcal{T}_V}\int_T \sigma_h^V : \nabla\boldsymbol{v}_h\,\mathrm{d}x\\
&\quad - \int_{\partial T}(\sigma_h^V)_{nt}\cdot(\boldsymbol{v}_h-\hat{\boldsymbol{v}}_h)_t\,\mathrm{d}s.
\end{aligned}$$

Applying Theorem 5.6 then shows that the right sum can further be written as

$$\begin{aligned}
&\sum_{V\in\mathcal{V}}\left(\sum_{T\in\mathcal{T}_V}\int_T \sigma_h^V : \nabla\boldsymbol{v}_h\,\mathrm{d}x - \int_{\partial T}(\sigma_h^V)_{nt}\cdot(\boldsymbol{v}_h-\hat{\boldsymbol{v}}_h)_t\,\mathrm{d}s\right)\\
&\qquad = \sum_{V\in\mathcal{V}} -\Big(\sum_{T\in\mathcal{T}_V}\int_T \boldsymbol{f}\cdot\boldsymbol{B}^V(\boldsymbol{v}_h) - \bar{\sigma}_h : \nabla\boldsymbol{B}^V(\boldsymbol{v}_h) + \bar{p}_h\operatorname{div}(\boldsymbol{B}^V(\boldsymbol{v}_h))\,\mathrm{d}x\\
&\qquad\qquad + \int_{\partial T}(\bar{\sigma}_h)_{nt}\cdot(\boldsymbol{B}^V(\boldsymbol{v}_h) - \phi_V\hat{\boldsymbol{v}}_h)_t\,\mathrm{d}s\Big)\\
&\qquad = -\sum_{T\in\mathcal{T}}\int_T \boldsymbol{f}\cdot\boldsymbol{v}_h\,\mathrm{d}x + \sum_{T\in\mathcal{T}}\int_T \bar{\sigma}_h : \nabla\boldsymbol{v}_h\,\mathrm{d}x - \int_{\partial T}(\bar{\sigma}_h)_{nt}\cdot(\boldsymbol{v}_h-\hat{\boldsymbol{v}}_h)_t\,\mathrm{d}s
\end{aligned}$$

where we used item *iii.* of Lemma 5.1 and $\operatorname{div}(\boldsymbol{v}_h) = 0$ in the last step. All together, this shows that

$$\sum_{T\in\mathcal{T}}\int_T \operatorname{div}(\sigma_h^{\mathsf{LEQ}})\cdot\boldsymbol{v}_h\,\mathrm{d}x - \sum_{F\in\mathcal{F}}\int_F [\![(\sigma_h^{\mathsf{LEQ}})_{nn}]\!](\boldsymbol{v}_h)_n\,\mathrm{d}s = -\sum_{T\in\mathcal{T}}\int_T \boldsymbol{f}\cdot\boldsymbol{v}_h\,\mathrm{d}x,$$

and we conclude the proof. □

6. Efficiency

This section proves efficiency of the proposed global and local equilibrated fluxes in the sense that the error estimator is a lower bound for the velocity error plus norms that only depend on the velocity and have the right order and data oscillations. In particular also the efficiency bound is pressure-independent.

Theorem 6.1 (Global efficiency of the global design)**.** The error estimator for $\sigma_h := \sigma_h^{\mathsf{MCS}}$ from (3.6), is efficient in the sense that

$$\eta(\sigma_h^{\mathsf{MCS}}) \lesssim \|\nabla(\boldsymbol{u}-\bar{\mathbf{u}}_h)\| + \nu^{-1}\|\sigma-\sigma_h^{\mathsf{MCS}}\| + \nu^{-1}h_T\operatorname{osc}_k(\operatorname{curl}(\boldsymbol{f}+\nu\Delta_{\mathcal{T}}\bar{\mathbf{u}}_h),\mathcal{T}).$$

The second term on the right-hand side can be estimated by Theorem 3.2 and may be of higher-order if the order of $\boldsymbol{V}_h$ is large enough and $\boldsymbol{u}$ is smooth enough. The third term on the right-hand side are oscillations as defined in [24] which may be of higher-order if $\boldsymbol{u}$ is smooth enough.

Proof. The proof employs the efficiency of the pressure-robust standard-residual based error estimator from [24]. Indeed, triangle inequalities to insert $\nabla\bar{\mathbf{u}}_h$ yield

$$\begin{aligned}\eta(\sigma_h)^2 =& \frac{1}{\nu^2}\sum_{T\in\mathcal{T}}\Big(c_1^2c_2^2h_T^2\|\operatorname{curl}(\boldsymbol{f}+\operatorname{div}(\sigma_h))\|_T + \|\operatorname{dev}(\sigma_h-\bar\sigma_h)\|_T\Big)^2\\ \lesssim& \frac{1}{\nu^2}\sum_{T\in\mathcal{T}}\Big(c_1^2c_2^2h_T^2\|\operatorname{curl}(\boldsymbol{f}+\operatorname{div}(\bar\sigma_h))\|_T + c_1^2c_2^2h_T^2\|\operatorname{curl}(\operatorname{div}(\sigma_h-\bar\sigma_h))\|_T + \|\operatorname{dev}(\sigma_h-\bar\sigma_h)\|_T\Big)^2.\end{aligned}$$

The efficiency of the first term follows from the efficiency proof for the pressure-robust residual estimator in [24], i.e.

$$\nu^{-1}h_T^2\|\operatorname{curl}_{\mathcal{T}}(\boldsymbol{f}+\nu\Delta_{\mathcal{T}}\bar{\mathbf{u}}_h)\|_T \lesssim \|\nabla(\boldsymbol{u}-\bar{\mathbf{u}}_h)\|_T + \nu^{-1}h_T\operatorname{osc}_k(\operatorname{curl}(\boldsymbol{f}+\nu\Delta_{\mathcal{T}}\bar{\mathbf{u}}_h),T).$$

Moreover, an inverse inequality shows

$$c_1^2c_2^2h_T^2\|\operatorname{curl}(\operatorname{div}(\sigma_h-\bar\sigma_h))\|_T \lesssim h_T\|\operatorname{div}(\sigma_h-\bar\sigma_h)\|_T \lesssim \|\sigma_h-\bar\sigma_h\|_T \leqslant \nu\|\nabla(\boldsymbol{u}-\bar{\mathbf{u}}_h)\|_T + \|\sigma-\sigma_h\|_T.$$

By another triangle inequality we have

$$\|\operatorname{dev}(\sigma_h-\bar\sigma_h)\|_T \leqslant \|\sigma_h-\bar\sigma_h\|_T \leqslant \nu\|\nabla(\boldsymbol{u}-\bar{\mathbf{u}}_h)\|_T + \|\sigma-\sigma_h\|_T.$$

The collection of all terms concludes the proof. □

Unfortunately local efficiency cannot be proven for the global design σ_h^{MCS}. However, the next theorem establishes also local efficiency bounds for the local design.

Theorem 6.2 (Local efficiency of the local design)**.** Let $\boldsymbol{v}_h \in \boldsymbol{V}_h$, with $\operatorname{div}\boldsymbol{v}_h = 0$, and $\hat{\boldsymbol{v}}_h \in \hat{\boldsymbol{V}}_h$ and assume that for each element $T \in \mathcal{T}$ we have $\Delta\boldsymbol{u} \in L^2(T)$. The local solution $(\sigma_h^V, (\tilde{\boldsymbol{u}}_h^V, \hat{\boldsymbol{u}}_h^V), p_h^V) \in \Sigma_h^V \times \boldsymbol{V}_h^V \times Q_h^V$ of (5.3) fulfills the (pressure-robust) estimate

$$\|\sigma_h^V\|_{\Sigma_h^V} \lesssim \left(\sum_{T\in\mathcal{T}_V}\|\sigma-\bar\sigma_h\|_T^2 + h_T\|(\nu\nabla\boldsymbol{u}-\nu\nabla\bar{\boldsymbol{u}}_h)_{nt}\|_{\partial T}^2\right)^{1/2} + \left(\sum_{T\in\mathcal{T}_V}h_T^2\|(\mathbf{id}-\boldsymbol{\pi}_{r-2})\nu\Delta\boldsymbol{u}\|_T^2\right)^{1/2}.$$

If the operator $\mathcal{R}$ of the primal method (3.1) is the identity, the last sum of the right hand side vanishes.

Proof. By Lemma 5.4, the inf-sup property of the bilinear form B on the subspace $\{\boldsymbol{v}_h^V = (\tilde{\boldsymbol{v}}_h^V, \hat{\boldsymbol{v}}_h^V) \in \boldsymbol{V}_h^V : \operatorname{div}(\tilde{\boldsymbol{v}}_h^V) = 0\}$ gives for the solution $(\sigma_h^V, \tilde{\boldsymbol{u}}_h^V, \hat{\boldsymbol{u}}_h^V)$ the estimate

$$\begin{aligned}\|\sigma_h^V\|_{\Sigma_h^V} + \|(\tilde{\boldsymbol{u}}_h^V, \hat{\boldsymbol{u}}_h^V)\|_{V_h^V} &\lesssim \sup_{\substack{(\tilde{\boldsymbol{v}}_h^V,\hat{\boldsymbol{v}}_h^V)\in\boldsymbol{V}_h^V\\ \operatorname{div}(\tilde{\boldsymbol{v}}_h^V)=0}} \frac{B((\sigma_h^V,\tilde{\boldsymbol{u}}_h^V,\hat{\boldsymbol{u}}_h^V,0),(\tau_h^V,\tilde{\boldsymbol{v}}_h^V,\hat{\boldsymbol{v}}_h^V,0))}{\|\tau_h^V\|_{\Sigma_h^V} + \|(\tilde{\boldsymbol{v}}_h^V,\hat{\boldsymbol{v}}_h^V)\|_{V_h^V}}\\ &\lesssim \sup_{\substack{(\tilde{\boldsymbol{v}}_h^V,\hat{\boldsymbol{v}}_h^V)\in\boldsymbol{V}_h^V\\ \operatorname{div}(\tilde{\boldsymbol{v}}_h^V)=0}} \frac{G_1^V(\boldsymbol{f},\bar{\boldsymbol{u}}_h,\bar p_h)(\tilde{\boldsymbol{v}}_h^V,\hat{\boldsymbol{v}}_h^V)}{\|(\tilde{\boldsymbol{v}}_h^V,\hat{\boldsymbol{v}}_h^V)\|_{V_h^V}}.\end{aligned}$$

Next with $\boldsymbol{f} = -\Delta\boldsymbol{u} + \nabla p$ and applying integration by parts (similar to (5.5)), the enumerator simplifies to

$$G_1^V(\boldsymbol{f},\bar{\boldsymbol{u}}_h,\bar p_h)(\tilde{\boldsymbol{v}}_h^V,\hat{\boldsymbol{v}}_h^V) = \sum_{T\in\mathcal{T}_V}\int_T(\sigma-\bar\sigma_h):\nabla\boldsymbol{B}^V(\tilde{\boldsymbol{v}}_h^V)\,\mathrm{d}x \tag{6.1}$$

$$-\sum_{T\in\mathcal{T}_V}\int_{\partial T}(\sigma-\bar\sigma_h)_{nt}(\boldsymbol{B}^V(\tilde{\boldsymbol{v}}_h^V)-\phi_V\hat{\boldsymbol{v}}_h^V)_t\,\mathrm{d}s \tag{6.2}$$

$$-\sum_{T\in\mathcal{T}_V}\int_T(p-\bar p_h)\operatorname{div}(\boldsymbol{B}^V(\tilde{\boldsymbol{v}}_h^V))\,\mathrm{d}x, \tag{6.3}$$

where we used that $\boldsymbol{B}^V(\tilde{\boldsymbol{v}}_h^V)\cdot\boldsymbol{n}=0$ on $\partial\omega_V$ (see item *i.* in Lemma 5.1) and that

$$\sum_{T\in\mathcal{T}_V}\int_{\partial T}\phi_V(\sigma)_{nt}\cdot(\hat{\boldsymbol{v}}_h^V)_t\,\mathrm{d}s=\sum_{F\in\mathcal{F}_V}\int_F[\![\phi_V(\sigma)_{nt}]\!]\cdot(\hat{\boldsymbol{v}}_h^V)_t\,\mathrm{d}s=0.$$

By the continuity of the bubble projector $\boldsymbol{B}^V$ (which reads as a weighting with ϕ_V) and that $\phi_V=\mathcal{O}(1)$ on ω_V, the Cauchy-Schwarz inequality applied to the sums in (6.1) and (6.2) gives

$$\begin{aligned}
&\sum_{T\in\mathcal{T}_V}\int_T(\sigma-\bar\sigma_h):\nabla\boldsymbol{B}^V(\tilde{\boldsymbol{v}}_h^V)\,\mathrm{d}x-\int_{\partial T}(\sigma-\bar\sigma_h)_{nt}(\boldsymbol{B}^V(\tilde{\boldsymbol{v}}_h^V)-\phi_V\hat{\boldsymbol{v}}_h^V)_t\,\mathrm{d}s\\
&\leqslant\sum_{T\in\mathcal{T}_V}\|(\sigma-\bar\sigma_h)\|_T\|\nabla\tilde{\boldsymbol{v}}_h^V\|_T+h_T\|(\sigma-\bar\sigma_h)_{nt}\|_{\partial T}\frac{1}{h_T}\|(\tilde{\boldsymbol{v}}_h^V-\hat{\boldsymbol{v}}_h^V)_t\|_{\partial T}\\
&\leqslant\left(\sum_{T\in\mathcal{T}_V}\|(\sigma-\bar\sigma_h)\|_T^2+h_T^2\|(\sigma-\bar\sigma_h)_{nt}\|_{\partial T}^2\right)^{1/2}\|(\tilde{\boldsymbol{v}}_h^V,\hat{\boldsymbol{v}}_h^V)\|_{V_h^V}.
\end{aligned}$$

We continue with the remaining third sum in (6.3) (which does not vanish, although $\tilde{\boldsymbol{v}}_h^V$ is divergence-free). For this let $\tilde p_h=\pi^{\bar Q_h}p$ be the L^2 projection of the exact pressure onto the pressure space $\bar Q_h$ and define the mean value

$$c_p=\frac{1}{|\mathcal{T}_V|}\sum_{T\in\mathcal{T}_V}\int_T(p-\bar p_h)\,\mathrm{d}x.$$

Since $\boldsymbol{B}^V(\tilde{\boldsymbol{v}}_h^V)\in\mathrm{BDM}^k(\mathcal{T}_V)$ according to property *ii.* in Lemma 5.1, we have that $\operatorname{div}(\boldsymbol{B}^V(\tilde{\boldsymbol{v}}_h^V))\in\bar Q_h$, which gives

$$\begin{aligned}
\sum_{T\in\mathcal{T}_V}\int_T(p-\bar p_h)\operatorname{div}(\boldsymbol{B}^V(\tilde{\boldsymbol{v}}_h^V))\,\mathrm{d}x&=\sum_{T\in\mathcal{T}_V}\int_T(\tilde p_h-\bar p_h)\operatorname{div}(\boldsymbol{B}^V(\tilde{\boldsymbol{v}}_h^V))\,\mathrm{d}x\\
&=\sum_{T\in\mathcal{T}_V}\int_T(\tilde p_h-\bar p_h-c_p)\operatorname{div}(\boldsymbol{B}^V(\tilde{\boldsymbol{v}}_h^V))\,\mathrm{d}x\\
&\lesssim\|\tilde p_h-\bar p_h-c_p\|_{\omega_V}\|(\tilde{\boldsymbol{v}}_h^V,\hat{\boldsymbol{v}}_h^V)\|_{V_h^V},
\end{aligned}$$

where we again used the continuity of $\boldsymbol{B}^V$. By the inf-sup condition of the primal Stokes discretization ($\tilde p_h-\bar p_h-c_p$ has a zero mean value) on the local space $\bar{\boldsymbol{V}}_h(\mathcal{T}_V):=\bar{\boldsymbol{V}}_h\cap H_0^1(\omega_V)$ we have

$$\|\tilde p_h-\bar p_h-c_p\|_{\omega_V}\lesssim\sup_{\bar{\boldsymbol{v}}_h\in\bar{\boldsymbol{V}}_h(\mathcal{T}_V)}\frac{\int_{\omega_V}(\tilde p_h-\bar p_h-c_p)\operatorname{div}(\bar{\boldsymbol{v}}_h)\,\mathrm{d}x}{\|\nabla\bar{\boldsymbol{v}}_h\|_{\omega_V}}.$$

Now, using that $\bar p_h$ is the discrete pressure solution we get

$$\begin{aligned}
-\int_{\omega_V}\bar p_h\operatorname{div}(\bar{\boldsymbol{v}}_h)\,\mathrm{d}x&=\int_{\omega_V}\boldsymbol{f}\cdot\mathcal{R}(\bar v_h)\,\mathrm{d}x-\int_{\omega_V}\nu\nabla\bar{\boldsymbol{u}}_h:\nabla\bar{\boldsymbol{v}}_h\,\mathrm{d}x\\
&=\int_{\omega_V}(-\nu\Delta\boldsymbol{u}+\nabla p)\cdot\mathcal{R}(\bar{\boldsymbol{v}}_h)\,\mathrm{d}x-\int_{\omega_V}\nu\nabla\bar{\boldsymbol{u}}_h:\nabla\bar{\boldsymbol{v}}_h\,\mathrm{d}x.
\end{aligned}$$

Since $\operatorname{div}(\mathcal{R}(\bar v_h))\in\bar Q_h$, see (3.4), we get using integration by parts

$$\int_{\omega_V}\nabla p\cdot\mathcal{R}(\bar{\boldsymbol{v}}_h)\,\mathrm{d}x=-\int_{\omega_V}p\operatorname{div}(\mathcal{R}(\bar{\boldsymbol{v}}_h))\,\mathrm{d}x=-\int_{\omega_V}\tilde p_h\operatorname{div}(\mathcal{R}(\bar{\boldsymbol{v}}_h))\,\mathrm{d}x=-\int_{\omega_V}\tilde p_h\operatorname{div}(\bar{\boldsymbol{v}}_h)\,\mathrm{d}x,$$

and so in total (since $\int_{\omega_V}c_p\operatorname{div}(\bar{\boldsymbol{v}}_h)\,\mathrm{d}x=0$ by Gauss's theorem)

$$\begin{aligned}
\int_{\omega_V}(\tilde p_h-\bar p_h-c_p)\operatorname{div}(\bar{\boldsymbol{v}}_h)\,\mathrm{d}x&=\int_{\omega_V}-\nu\Delta\boldsymbol{u}\cdot\mathcal{R}(\bar{\boldsymbol{v}}_h)\,\mathrm{d}x-\int_{\omega_V}\bar\sigma_h:\nabla\bar{\boldsymbol{v}}_h\,\mathrm{d}x\\
&=\int_{\omega_V}-\nu\Delta\boldsymbol{u}\cdot(\mathcal{R}(\bar{\boldsymbol{v}}_h)-\bar{\boldsymbol{v}}_h)\,\mathrm{d}x+\int_{\omega_V}(\sigma-\bar\sigma_h):\nabla\bar{\boldsymbol{v}}_h\,\mathrm{d}x,
\end{aligned}$$

where we added and subtracting (including integration by parts) $\int_{\omega_V} \sigma : \nabla \bar{\boldsymbol{v}}_h \,\mathrm{d}x$. By the properties of the reconstruction operator, the first integral can be bounded by

$$\int_{\omega_V} -\nu\Delta \boldsymbol{u} \cdot (\mathcal{R}(\bar{\boldsymbol{v}}_h) - \bar{\boldsymbol{v}}_h)\,\mathrm{d}x \lesssim \|(\mathbf{id} - \boldsymbol{\pi}_{\omega_V}^{r-2})\nu\Delta \boldsymbol{u}\|_{\omega_V} h_V \|\nabla \bar{\boldsymbol{v}}_h\|_{\omega_V}, \tag{6.4}$$

where h_V denotes the diameter of the vertex patch ω_V. Thus by the Cauchy Schwarz inequality we get the estimate

$$\|\tilde{p}_h - \bar{p}_h - c_p\|_{\omega_V} \lesssim h_V \|(\mathbf{id} - \boldsymbol{\pi}_{\omega_V}^{r-2})\nu\Delta \boldsymbol{u}\|_{\omega_V} + \left(\sum_{T\in\mathcal{T}_V} \|(\sigma - \bar{\sigma}_h)\|_T^2\right)^{1/2},$$

and so

$$\begin{aligned} G_1^V(\boldsymbol{f}, \bar{\boldsymbol{u}}_h, \bar{p}_h)(\tilde{\boldsymbol{v}}_h^V, \hat{\boldsymbol{v}}_h^V) \lesssim \left(\sum_{T\in\mathcal{T}_V} \|(\sigma - \bar{\sigma}_h)\|_T^2 + h_T^2 \|(\sigma - \bar{\sigma}_h)_{nt}\|_{\partial T}^2\right)^{1/2} \|(\tilde{\boldsymbol{v}}_h^V, \hat{\boldsymbol{v}}_h^V)\|_{V_h^V} \\ + h_V \|(\mathbf{id} - \boldsymbol{\pi}_{\omega_V}^{r-2})\nu\Delta \boldsymbol{u}\|_{\omega_V} \|(\tilde{\boldsymbol{v}}_h^V, \hat{\boldsymbol{v}}_h^V)\|_{V_h^V}. \end{aligned}$$

This concludes the proof for the general case. Now assume that $\mathcal{R} = \mathbf{id}$, then we see that the additional term in (6.4) vanishes which proves the stated result in the case where no reconstruction operator in the primal method (3.1) is included. □

7. Numerical Examples

This section confirms the theoretical results by some numerical examples. For the ease of representation we introduce the following notation. We denote by η^N the estimator of Theorem 4.1 where $\sigma_h = \sigma_h^N$ is the solution of the mixed system given in Remark 4.2 with $q_1 = 0$ and $q_2 = \bar{p}_h$. The pressure-robust estimator of Theorem 4.5 is denoted by η. Here, the flux σ_h either corresponds to the solution σ_h^{MCS} of the global problem (3.6) or to the local equilibrated flux σ_h^{LEQ} given by equation (5.7). Further, we define the contributions

$$\begin{aligned} \eta_{\mathbf{f}} &= \nu^{-1}\|h_T(\mathbf{id} - \pi_{k-2})\,\mathrm{curl}(\mathbf{f} + \mathrm{div}(\sigma_h)\|, & \eta_{\mathbf{f}}^N &= (\nu\pi)^{-1}\|h_T\mathbf{f} - \mathrm{div}(\sigma_h^N)\|, \\ \eta_\sigma &= \nu^{-1}\|\,\mathrm{dev}(\sigma_h - \bar{\sigma}_h)\|, & \eta_\sigma^N &= \nu^{-1}\|\sigma_h^N + \bar{p}_h I_{d\times d} - \bar{\sigma}_h\|, \\ \eta_{\mathrm{div}} &= c_0^{-1}\|(\mathrm{div}(\bar{\boldsymbol{u}}_h)\|. \end{aligned}$$

Table 7.1 shows the different inf-sup stable velocity pressure pairs that we consider for the primal formulation (3.1). Further we give the abbreviation that we use, the expected convergence rate of the error r and the used reconstruction operator in (3.1) that ensures pressure-robustness. The order $k = r$ also corresponds to the order of the reconstruction space $\boldsymbol{V}_h = \mathrm{RT}_k$ and the order of the spaces used in the equilibration designs (3.6) and (5.7). Moreover in two dimensions, $\boldsymbol{P}_{2,c,+}$ denotes the space of vector-valued polynomials of order 2 including the local cubic element bubbles, i.e.

$$\boldsymbol{P}_{2,c,+}(\mathcal{T}) := \{q \in \boldsymbol{P}_{3,c}(\mathcal{T}) : q|_F \in \boldsymbol{P}_2(F) \forall F \in \mathcal{F}\}.$$

In three dimension, we similarly denote by $\boldsymbol{P}_{2,c,+}^{\mathsf{3d}}$ the space of vector-valued polynomials of order 2 including the local element bubbles of order 4 and the cubic face bubbles of order 3. A precise definition is given in example 8.7.2 in [3].

The adaptive mesh refinement loop is defined as usual by

$$\mathrm{SOLVE} \to \mathrm{ESTIMATE} \to \mathrm{MARK} \to \mathrm{REFINE} \to \mathrm{SOLVE} \to \ldots$$

and employs the local contributions to the error estimator as element-wise refinement indicators. In the marking step, an element $T \in \mathcal{T}$ is marked for refinement if $\eta(T) \geqslant \frac{1}{4}\max_{K\in\mathcal{T}} \eta(K)$. The refinement step refines all marked elements plus further elements in a closure step to guarantee a regular triangulation.

$\bar{\boldsymbol{V}}_h \times \bar{Q}_h$	abbr.	$r = k$	$\mathcal{R}$
$\boldsymbol{P}_{2,c}(\mathcal{T}) \times P_0(\mathcal{T})$	P20	1	I_{BDM_1}
$\boldsymbol{P}_{3,c}(\mathcal{T}) \times P_1(\mathcal{T})$	P31	2	I_{BDM_2}
$\boldsymbol{P}_{2,c,+}(\mathcal{T}) \times P_1(\mathcal{T})$	P2B	2	I_{BDM_2}
$\boldsymbol{P}^{\mathsf{3d}}_{2,c,+}(\mathcal{T}) \times P_1(\mathcal{T})$	P2B-3d	2	I_{BDM_2}
$\boldsymbol{P}_{2,c}(\mathcal{T}) \times P_1(\mathcal{T})$	SV	2	$\mathbf{id}$

TABLE 7.1. Considered inf-sup stable Stokes pairs including the expected order of convergence and the used reconstruction operator.

In the case of the Scott-Vogelius (SV) finite element approximation, the adaptive algorithm includes two meshes: the macro element mesh $\mathcal{T}$ given by a standard triangulation, and the corresponding barycentric refined triangulation (guaranteeing inf-sup stability of the SV element) denoted by $\mathcal{T}_{\mathrm{bar}}(\mathcal{T})$. Again, an element $T \in \mathcal{T}$ is marked if (mean value of the elements included in one macro element)

$$\frac{1}{3} \sum_{\substack{T' \in \mathcal{T}_{\mathrm{bar}} \\ T' \cap T \neq \emptyset}} \mu(T') \geqslant \frac{1}{4} \max_{K \in \mathcal{T}_{\mathrm{bar}}} \eta(K).$$

The refinement of $\mathcal{T}$ is done as described before. The final mesh is then obtained by a global barycentric refinement step. Note, that although the macro element meshes are nested, there barycentric refinement are in general not nested.

The implementation and numerical examples where performed with the finite element library NGSolve/Netgen [38, 37], see also www.ngsolve.org.

	ref. level	0	1	2	3	4
$\nu = 1$	$\sigma_h = \sigma_h^N$	2.62	2.43	2.29	2.20	2.15
$\nu = 1$	$\sigma_h = \sigma_h^{\mathsf{MCS}}$	2.30	1.75	1.29	1.14	1.07
$\nu = 1$	$\sigma_h = \sigma_h^{\mathsf{LEQ}}$	3.08	2.48	2.01	1.81	1.70
$\nu = 10^{-4}$	$\sigma_h = \sigma_h^N$	$9.53 \cdot 10^3$	$1.15 \cdot 10^4$	$9.66 \cdot 10^3$	$9.63 \cdot 10^3$	$9.75 \cdot 10^3$
$\nu = 10^{-4}$	$\sigma_h = \sigma_h^{\mathsf{MCS}}$	2.30	1.75	1.29	1.14	1.07
$\nu = 10^{-4}$	$\sigma_h = \sigma_h^{\mathsf{LEQ}}$	3.08	2.48	2.01	1.81	1.70

TABLE 7.2. Efficiency indices in Example 1 on uniformly refined meshes and the SV element.

7.1. **Smooth example on unit square.** The first example considers the Stokes problem on a unit square domain $\Omega = (0,1)^2$ with the smooth prescribed solution

$$\boldsymbol{u}(x,y) := \operatorname{curl}\left(x^2(1-x)^2y^2(1-y)^2\right) \quad \text{and} \quad p(x,y) := x^5 + y^5 - 1/3$$

with matching right-hand side $\boldsymbol{f} := -\nu\Delta\boldsymbol{u} + \nabla p$ for variable viscosity ν.

Figure 7.1 presents the convergence history of the error of the discrete Stokes solution $\bar{\boldsymbol{u}}_h$ measured in the H^1-semi norm using the SV element with two different viscosities $\nu = 1$ (top) and $\nu = 10^{-4}$ (bottom) on uniformly refined meshes. The first important observation is that the error plot for the pressure-robust error estimator σ_h^{MCS} looks exactly the same for $\nu = 1$ and $\nu = 10^{-4}$, while the 'naive' estimator σ_h^N is nowhere close to the exact error of the pressure-robust Scott-Vogelius solution for $\nu = 10^{-4}$. As expected, the error estimator scales with ν^{-1} and so does its efficiency index. One can also see, that the volume term $\eta_{\boldsymbol{f}}^N$ is of higher order, nevertheless even on the finest mesh it is still larger than the full pressure-robust error estimator. Further, even if this quantity would be small, also η_σ^N is inefficient. To sum up, the classical error estimator approach is not very efficient for pressure-robust or divergence-free discretisations in pressure-dominant situations (meaning $\nu^{-1}p$ is large compared to $\boldsymbol{u}$).

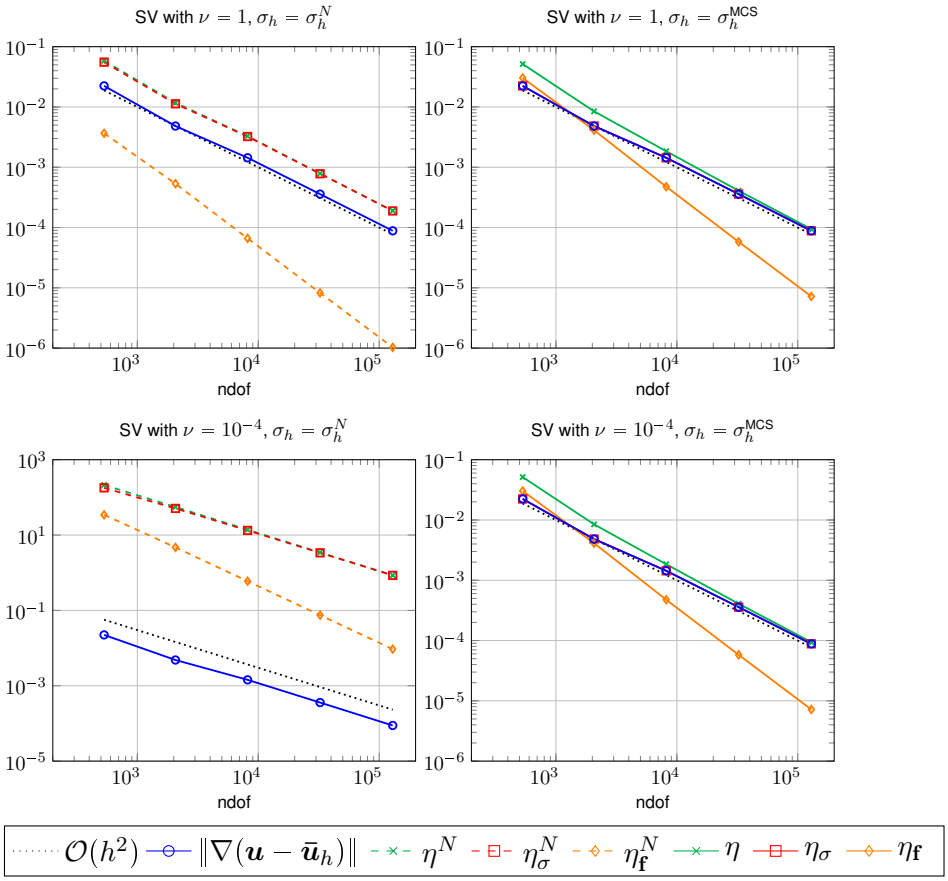

FIGURE 7.1. Example 1: Convergence history of exact error and error estimator quantities on uniformly refined meshes for SV with $\nu = 1$ (top) and 10^{-4} (bottom) and $\sigma = \sigma_h^N$ (left) and $\sigma = \sigma_h^{\mathrm{MCS}}$ (right).

Table 7.2 lists the efficiency indices on the different refinement levels also for the pressure-robust local variant of our error estimator. One can see that the error estimator for σ_h^{MCS} even is asymptotically exact, while the local variant is not, but still attains very good efficiency indices around 2. We want to mention again that our error bounds, unfortunately, contain unknown constants c_1 and c_2 which were evaluated by $c_1 c_2 = 1$. However, they only appear in front of $\eta_{\boldsymbol{f}}$ which is, at least in this example and for uniform mesh refinement, of higher order (see Figure 7.1 again).

7.2. **Smooth example on unit cube.** The second example is an extension of the previous example onto the unit cube $\Omega = (0,1)^3$. Similarly, the smooth prescribed solution is now given by

$$\boldsymbol{u}(x,y) := \operatorname{curl}(\xi,\xi,\xi) \quad \text{and} \quad p(x,y) := x^5 + y^5 + z^5 - 1/2$$

with the potential $\xi = x^2(1-x)^2y^2(1-y)^2z^2(1-z)^2$ and with matching right-hand side $\boldsymbol{f} := -\nu\Delta\boldsymbol{u} + \nabla p$ for variable viscosity ν.

Figure 7.2 presents the convergence history of the error of the discrete Stokes solution $\bar{\boldsymbol{u}}_h$ measured in the H^1-semi norm using the P2B-3d element with two different viscosities $\nu = 1$ (top) and $\nu = 10^{-4}$ (bottom) on uniformly refined meshes. We can make similar observations as for the two dimensionsl case which validates our results also for the case $d = 3$. Further note, that since the right-hand side $\boldsymbol{f}$ is a polynomial of higher order compared to the two dimensional example, the oscillation terms $\eta_{\boldsymbol{f}}, \eta_{\boldsymbol{f}}^N$ are much larger and dominating the error estimator at coarser levels.

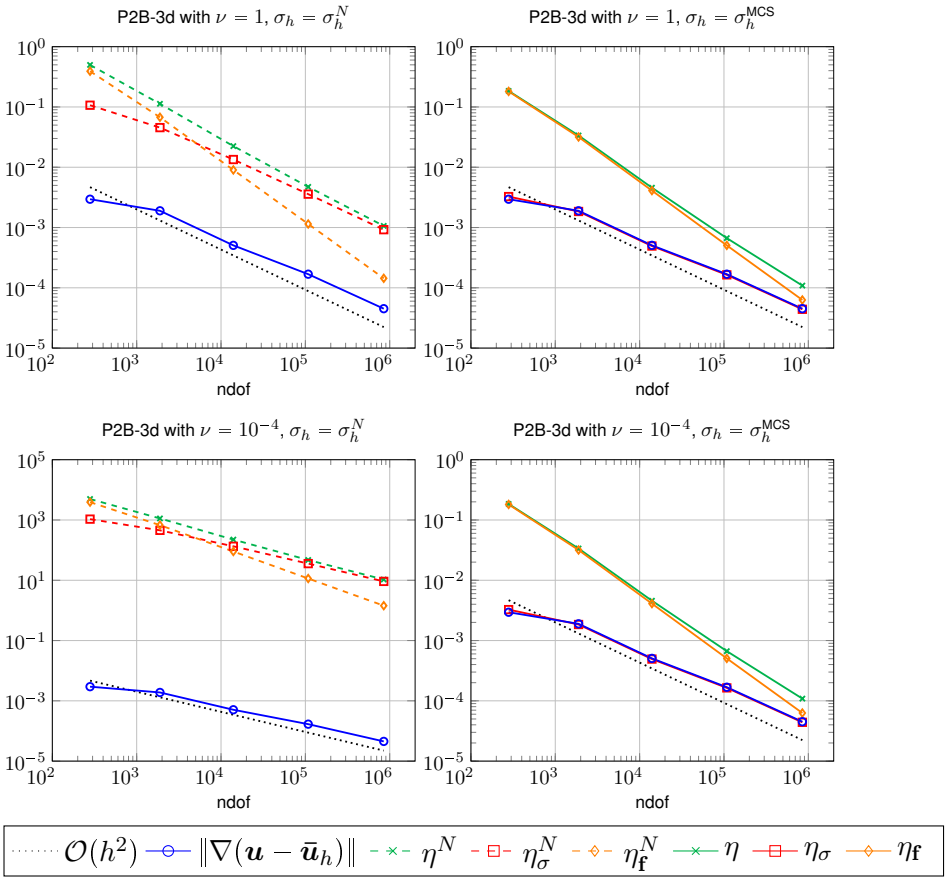

FIGURE 7.2. Example 2: Convergence history of exact error and error estimator quantities on uniformly refined meshes for P2B-3d with $\nu = 1$ (top) and 10^{-4} (bottom) and $\sigma = \sigma_h^N$ (left) and $\sigma = \sigma_h^{\mathrm{MCS}}$ (right).

7.3. **L-shaped domain example.** We consider the example from [40] given on the L-shaped domain $\Omega := (-1,1)^2 \backslash \big((0,1) \times (-1,0)\big)$. The velocity $\boldsymbol{u}$ and pressure p_0 now satisfy $-\nu\Delta\boldsymbol{u} + \nabla p_0 = 0$, and read as (given in polar coordinates with radius R and angle φ)

$$\boldsymbol{u}(R,\varphi) := R^\alpha \begin{pmatrix} (\alpha+1)\sin(\varphi)\psi(\varphi) + \cos(\varphi)\psi'(\varphi) \\ -(\alpha+1)\cos(\varphi)\psi(\varphi) + \sin(\varphi)\psi'(\varphi) \end{pmatrix}^T,$$
$$p_0 := \nu R^{(\alpha-1)}((1+\alpha)^2\psi'(\varphi) + \psi'''(\varphi))/(1-\alpha)$$

with

$$\psi(\varphi) := 1/(\alpha+1)\ \sin((\alpha+1)\varphi)\cos(\alpha\omega) - \cos((\alpha+1)\varphi) \\ - 1/(\alpha-1)\ \sin((\alpha-1)\varphi)\cos(\alpha\omega) + \cos((\alpha-1)\varphi)$$

and $\alpha = 856399/1572864 \approx 0.54$, $\omega = 3\pi/2$. To have a nonzero right-hand side we add the pressure $p_+ := \sin(xy\pi)$, i.e. $p := p_0 + p_+$ and $\boldsymbol{f} := \nabla(p_+)$. Note that, since $\boldsymbol{f}$ is a gradient, it holds $\eta_{\boldsymbol{f}} = 0$ in this example.

Figure 7.3 shows the convergence history of the exact error and the error estimators based on the naive equilibrated fluxes σ_h^N and the pressure-robust flxes σ_h^{MCS} on adaptively refined meshes where the refinement indicators are steered by the local contributions of the estimators. For $\nu = 1$ both estimators are efficient, the pressure-robust one is even asmyptotically exact, and all convergence rates are optimal. For $\nu = 10^{-4}$ the numbers and meshes for the pressure-robust estimator are exactly the same (which is fine, since the deiscrete velocity did not change), but the adaptive meshes for the naive estimator do not refine the corner singularity and therefore fail to reduce

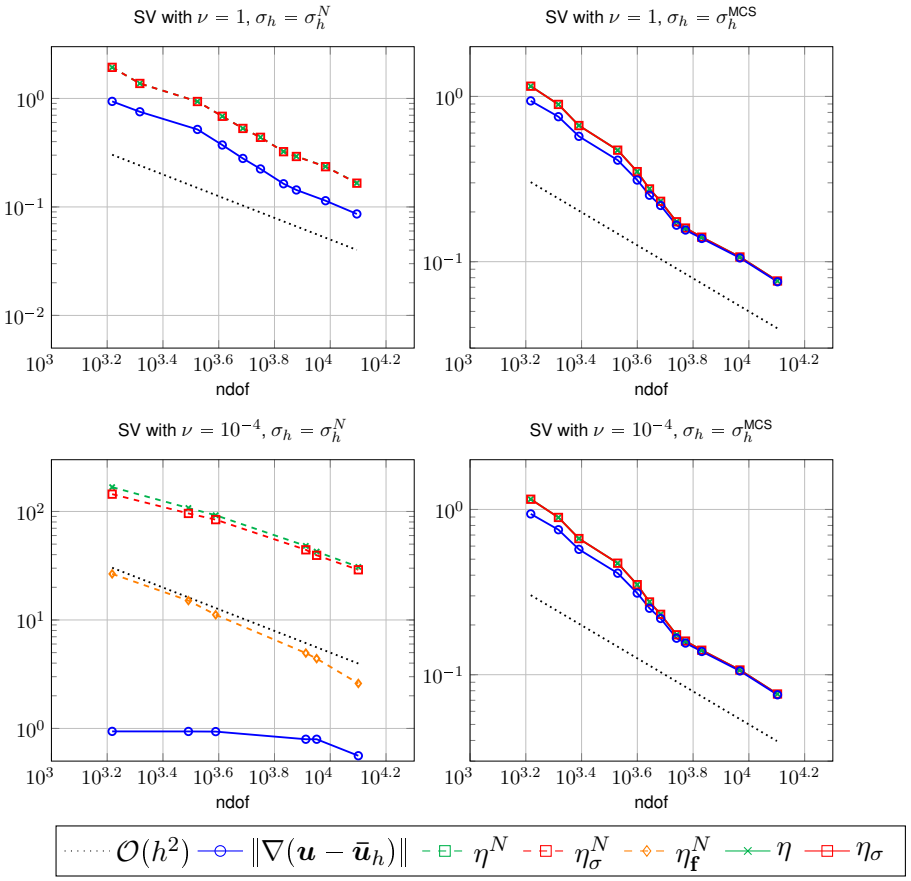

FIGURE 7.3. Example 3: Convergence history of exact error and error estimator quantities on adaptively refined meshes for SV with $\nu = 1$ (top) and 10^{-4} (bottom) and $\sigma_h = \sigma_h^N$ (left) and $\sigma_h = \sigma_h^{\mathrm{MCS}}$ (right).

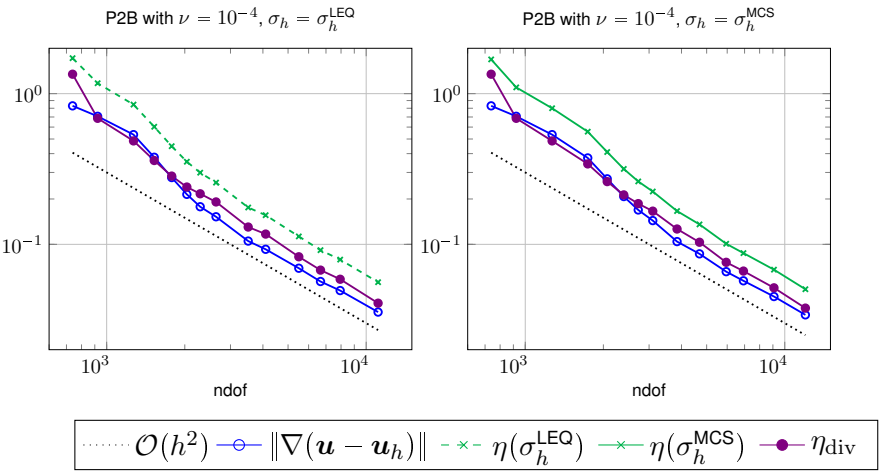

FIGURE 7.4. Example 3: Convergence history of exact error and error estimator quantities on adaptively refined meshes for P2B with 10^{-4} and $\sigma_h = \sigma_h^{\mathrm{LEQ}}$ (left) and $\sigma_h = \sigma_h^{\mathrm{MCS}}$ (right).

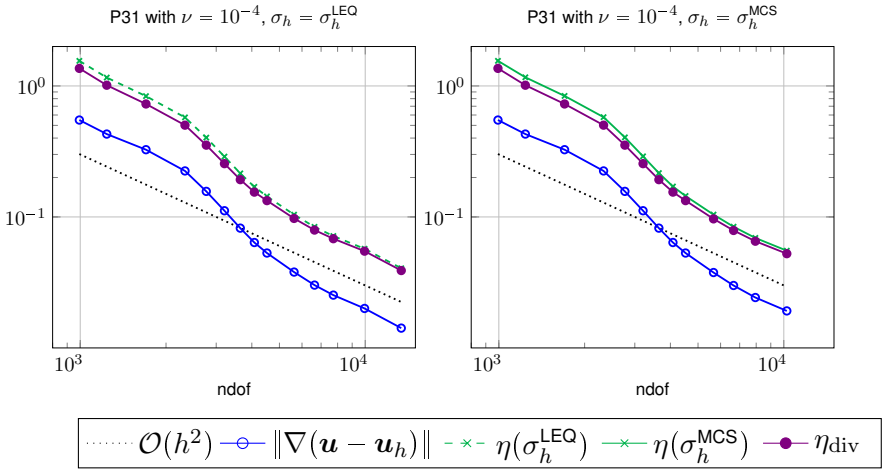

FIGURE 7.5. Example 3: Convergence history of exact error and error estimator quantities on adaptively refined meshes for P31 with 10^{-4} and $\sigma_h = \sigma_h^{\mathrm{LEQ}}$ (left) and $\sigma_h = \sigma_h^{\mathrm{MCS}}$ (right).

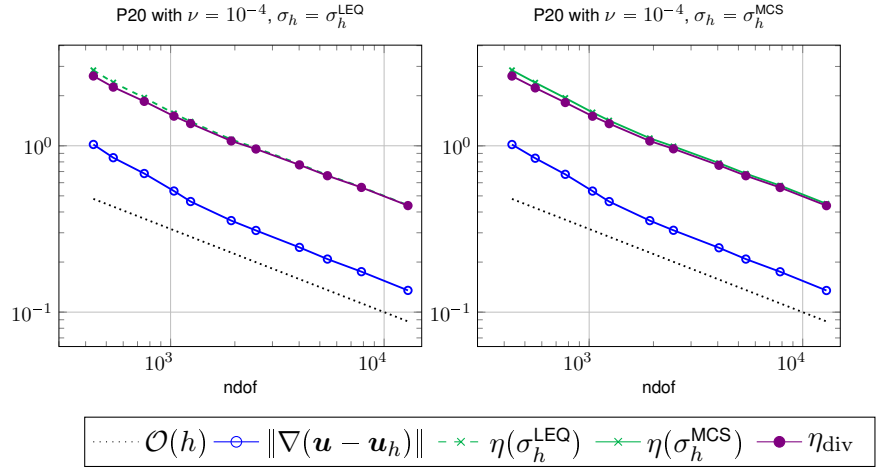

FIGURE 7.6. Example 3: Convergence history of exact error and error estimator quantities on adaptively refined meshes for P20 with 10^{-4} and $\sigma_h = \sigma_h^{\mathrm{LEQ}}$ (left) and $\sigma_h = \sigma_h^{\mathrm{MCS}}$ (right).

	ref. level	$\mathrm{ref}_{\mathrm{tot}} - 4$	$\mathrm{ref}_{\mathrm{tot}} - 3$	$\mathrm{ref}_{\mathrm{tot}} - 2$	$\mathrm{ref}_{\mathrm{tot}} - 1$	$\mathrm{ref}_{\mathrm{tot}}$
$\nu = 1$	$\sigma_h = \sigma_h^N$	1.96	1.98	2.04	2.07	1.93
$\nu = 1$	$\sigma_h = \sigma_h^{\mathrm{MCS}}$	1.05	1.03	1.02	1.01	1.01
$\nu = 1$	$\sigma_h = \sigma_h^{\mathrm{LEQ}}$	1.61	1.63	1.69	1.62	1.60
$\nu = 10^{-4}$	$\sigma_h = \sigma_h^N$	$1.15 \cdot 10^2$	$9.87 \cdot 10^1$	$6.05 \cdot 10^1$	$5.36 \cdot 10^1$	$5.50 \cdot 10^1$
$\nu = 10^{-4}$	$\sigma_h = \sigma_h^{\mathrm{MCS}}$	1.05	1.03	1.02	1.01	1.01
$\nu = 10^{-4}$	$\sigma_h = \sigma_h^{\mathrm{LEQ}}$	1.61	1.63	1.69	1.62	1.60

TABLE 7.3. Efficiency indices in Example 3 on adaptive refined meshes using the SV element. Here $\mathrm{ref}_{\mathrm{tot}}$ denotes the total number of refinement steps of each calculation.

the velocity error. Here, the refinement indicators only see the dominating pressure error and mark accordingly to reduce the pressure error. Adaptation to the corner singularity only starts when both pressure error times ν^{-1} and velocity error are on par. This behaviour was also observed in [24].

Figures 7.4-7.6 display results for the three other methods P2B, P31 and P20 for the local and global varaint of our pressure-robust error estimator. Since, the discrete velocity and the error estimator is independent of ν, we only show the results for $\nu = 10^{-4}$. Note, that these methods are not divergence-free but pressure-robust due to their reconstruction operator in the right-hand side. However, this causes $\mathrm{div}(\boldsymbol{u}_h) \neq 0$ and hence the contribution η_{div} appears here. Unfortunately, due to the constant $1/c_0$ in front of this term, it has a significant impact on the efficiency of the error estimator that is largest for P20 and smallest for P2B leading to still very small efficiency indices between 1.5 and 3 for both the local and the global equilibration error estimator.

ACKNOWLEDGEMENTS

Philip L. Lederer has been funded by the Austrian Science Fund (FWF) through the research programm “Taming complexity in partial differential systems” (F65) - project “Automated discretization in multiphysics” (P10).

REFERENCES

1. M. Ainsworth and W. Dörfler, *Reliable a posteriori error control for nonconformal finite element approximation of Stokes flow*, Math. Comp. **74** (2005), no. 252, 1599–1619 (electronic).
2. F. Bertrand and D. Boffi, *The prager-synge theorem in reconstruction based a posteriori error estimation*, 2019.
3. Daniele Boffi and Lucia Gastaldi (eds.), *Mixed Finite Elements, Compatibility Conditions, and Applications*, Lecture Notes in Mathematics, vol. 139, Springer, April 2008.
4. D. Braess and J. Schöberl, *Equilibrated residual error estimator for edge elements*, Math. Comp. **77** (2008), 651–672.
5. P. Bringmann, C. Carstensen, and C. Merdon, *Guaranteed velocity error control for the pseudostress approximation of the stokes equations*, Numerical Methods for Partial Differential Equations **32** (2016).
6. C. Carstensen, M. Eigel, R. H. W. Hoppe, and C. LÃűbhard, *A review of unified a posteriori finite element error control*, Numerical Mathematics: Theory, Methods and Applications **5** (2012), no. 4, 509âĂŞ558.
7. Carsten Carstensen and Christian Merdon, *Computational Survey on A Posteriori Error Estimators for the Crouzeix–Raviart Nonconforming Finite Element Method for the Stokes Problem*, Comput. Methods Appl. Math. **14** (2014), no. 1, 35–54. MR 3149616
8. M. Costabel and A. McIntosh, *On Bogovskiĭ and regularized Poincaré integral operators for de Rham complexes on Lipschitz domains*, Mathematische Zeitschrift **265** (2010), no. 2, 297–320.
9. L. Demkowicz, P. Monk, L. Vardapetyan, and W. Rachowicz, *De rham diagram for hp finite element spaces*, Computers & Mathematics with Applications **39** (2000), no. 7, 29 – 38.
10. P. Destuynder and B. Métivet, *Explicit error bounds in a conforming finite element method*, Mathematics of Computation **68** (1999), 1379–1396.
11. A. Ern and M. Vohralík, *Polynomial-degree-robust a posteriori estimates in a unified setting for conforming, nonconforming, discontinuous galerkin, and mixed discretizations*, SIAM Journal on Numerical Analysis **53** (2015), no. 2, 1058–1081.
12. R. Falk and M. Neilan, *Stokes complexes and the construction of stable finite elements with pointwise mass conservation*, SIAM J. Numer. Anal. **51** (2013), no. 2, 1308–1326. MR 3045658
13. J. Gedicke, S. Geevers, I. Perugia, and J. Schöberl, *A polynomial-degree-robust a posteriori error estimator for Nédélec discretizations of magnetostatic problems*, 2020.
14. J. Gopalakrishnan, P.L. Lederer, and J. Schöberl, *A mass conserving mixed stress formulation for Stokes flow with weakly imposed stress symmetry*, SIAM J. Numer. Anal., To appear.
15. J. Gopalakrishnan, P.L. Lederer, and J. Schöberl, *A mass conserving mixed stress formulation for the Stokes equations*, IMA Journal of Numerical Analysis (2019).
16. J. Guzmán and M. Neilan, *Conforming and divergence-free Stokes elements on general triangular meshes*, Math. Comp. **83** (2014), no. 285, 15–36. MR 3120580
17. A. Hannukainen, R. Stenberg, and M. Vohralík, *A unified framework for a posteriori error estimation for the Stokes problem*, Numer. Math. **122** (2012), no. 4, 725–769. MR 2995179
18. V. John, A. Linke, C. Merdon, M. Neilan, and L. Rebholz, *On the divergence constraint in mixed finite element methods for incompressible flows*, SIAM Review **59** (2017), no. 3, 492–544.
19. G. Kanschat and N. Sharma, *Divergence-conforming discontinuous galerkin methods and c^0 interior penalty methods*, SIAM Journal on Numerical Analysis **52** (2014), no. 4, 1822–1842.
20. C. Kreuzer, R. Verfürth, and P. Zanotti, *Quasi-optimal and pressure robust discretizations of the stokes equations by moment- and divergence-preserving operators*, 2020.
21. P. Lederer, A. Linke, C. Merdon, and J. Schöberl, *Divergence-free reconstruction operators for pressure-robust stokes discretizations with continuous pressure finite elements*, SIAM Journal on Numerical Analysis **55** (2017), no. 3, 1291–1314.
22. P.L. Lederer, *A mass conserving mixed stress formulation for incompressible flows*, Ph.D. thesis, Technical University of Vienna, 2019.
23. P.L. Lederer, C. Lehrenfeld, and J. Schöberl, *Hybrid discontinuous galerkin methods with relaxed h(div)-conformity for incompressible flows. part i*, SIAM Journal on Numerical Analysis **56** (2018), no. 4, 2070–2094.

24. P.L. Lederer, C. Merdon, and J. Schöberl, *Refined a posteriori error estimation for classical and pressure-robust stokes finite element methods*, Numerische Mathematik **142** (2019), no. 3, 713–748.
25. A. Linke, *On the role of the Helmholtz decomposition in mixed methods for incompressible flows and a new variational crime*, Comput. Methods Appl. Mech. Engrg. **268** (2014), 782–800. MR 3133522
26. A. Linke, G. Matthies, and L. Tobiska, *Robust arbitrary order mixed finite element methods for the incompressible stokes equations with pressure independent velocity errors*, ESAIM: M2AN **50** (2016), no. 1, 289–309.
27. A. Linke and C. Merdon, *Guaranteed energy error estimators for a modified robust Crouzeix-Raviart Stokes element*, J. Sci. Comput. **64** (2015), no. 2, 541–558. MR 3366087
28. _____, *Pressure-robustness and discrete Helmholtz projectors in mixed finite element methods for the incompressible Navier-Stokes equations*, Comput. Methods Appl. Mech. Engrg. **311** (2016), 304–326. MR 3564690
29. A. Linke, C. Merdon, and M. Neilan, *Pressure-robustness in quasi-optimal a priori estimates for the Stokes problem*, 281–294 (de), Online available: https://epub.oeaw.ac.at/?arp=0x003b8d45.
30. R. Luce and B. Wohlmuth, *A local a posteriori error estimator based on equilibrated fluxes*, SIAM J. Numer. Anal. **42** (2004), 1394–1414.
31. J. M. Melenk and C. Rojik, *On commuting p-version projection-based interpolation on tetrahedra*, Mathematics of Computation **89** (2019), no. 321, 45–87.
32. C. Merdon, *Aspects of guaranteed error control in computations for partial differential equations*, Ph.D. thesis, Humboldt-Universität zu Berlin, 2013.
33. P. Monk, *Finite element methods for Maxwell's equations*, Numerical Mathematics and Scientific Computation, Oxford University Press, New York, 2003. MR 2059447 (2005d:65003)
34. P. Neittaanmäki and S. Repin, *A posteriori error majorants for approximations of the evolutionary stokes problem*, Journal of Numerical Mathematics **18** (2010), no. 2, 119 – 134.
35. W. Prager and J. L. Synge, *Approximations in elasticity based on the concept of function space*, Quart. Appl. Math. **5** (1947), 241–269. MR 0025902
36. S.I. Repin, *A posteriori estimates for partial differential equations*, De Gruyter, Berlin, Boston, 2008.
37. J. Schöberl, *NETGEN An advancing front 2D/3D-mesh generator based on abstract rules*, Computing and Visualization in Science **1** (1997), no. 1, 41–52.
38. _____, *C++11 Implementation of Finite Elements in NGSolve*, Institute for Analysis and Scientific Computing, Vienna University of Technology (2014).
39. L. R. Scott and M. Vogelius, *Conforming finite element methods for incompressible and nearly incompressible continua*, Large-scale computations in fluid mechanics, Part 2 (La Jolla, Calif., 1983), Lectures in Appl. Math., vol. 22, Amer. Math. Soc., Providence, RI, 1985, pp. 221–244. MR 818790 (87h:65202)
40. R. Verfürth, *A posteriori error estimators for the Stokes equations*, Numer. Math. **55** (1989), no. 3, 309–325. MR 993474
41. J. Wang, Y. Wang, and X. Ye, *Unified a posteriori error estimator for finite element methods for the Stokes equations*, Int. J. Numer. Anal. Model. **10** (2013), no. 3, 551–570. MR 3064266
42. L. Zhao, E.J. Park, and E. Chung, *A pressure robust staggered discontinuous Galerkin method for the Stokes equations*, 2020.